HILGARDIA

A JOURNAL OF AGRICULTURAL SCIENCE PUBLISHED BY THE CALIFORNIA AGRICULTURAL EXPERIMENT STATION

Volume 51, Number 1 • April, 1983

Annual Grassland Ecosystem Model

Dennis F. Pendleton, John W. Menke, William A. Williams, and Robert G. Woodmansee

UNIVERSITY OF CALIFORNIA DIVISION OF AGRICULTURAL SCIENCES

A dynamic computer model of the annual grassland ecosystem of California (ELMAGE) has been developed through the adaptation of ELM, a compartment/flow computer model constructed in the US/IBP Grassland Biome. The modeling effort was part of a larger project involving an interdisciplinary team of researchers with the objective of compiling and synthesizing diverse information on the annual grassland ecosystem. Primary data from the San Joaquin Experimental Range and other information from published and unpublished sources were used in developing the model.

The general objective was to simulate the seasonal dynamics of biomass in the annual grassland on a daily basis. The components of the grassland ecosystem—weather factors, primary producers, decomposers, nutrients, and mammalian consumers—are described in linked submodels. Process mechanisms in each of the submodels control flow rates of carbon (biomass), nutrients, and water through the simulated system. Driving variables are temperature, precipitation, relative humidity, wind speed, and cloud cover.

Specific model objectives included assessment of the effect of changes in weather factors, fertilization practices, seeding practices, and stocking level of livestock on forage production and botanical composition of a simulated site. Implicit goals of the work included the use of the model to facilitate organization of information on the annual grassland, to test hypotheses concerning poorly understood biological phenomena, and to suggest future research needs.

THE AUTHORS:

Dennis F. Pendleton is Program Specialist, University Extension, Davis. John W. Menke is Associate Professor, Department of Agronomy and Range Science, Davis. William A. Williams is Professor, Department of Agronomy and Range Science, Davis. Robert G. Woodmansee is Associate Professor, Department of Range Science, Colorado State University, Fort Collins.

Dennis F. Pendleton, John W. Menke, William A. Williams, and Robert G. Woodmansee

Annual Grassland Ecosystem Model[1]

INTRODUCTION

A SIMULATION MODEL of a representative community in the annual grasslands of California (ELMAGE) was developed through the adaptation of ELM, a model of the short-grass prairie constructed in the US/IBP Grassland Biome (Innis, 1978). Until this effort, ELM had been applied exclusively to communities dominated by perennial plants. The basic structure of the ELMAGE model is the same as that of ELM, although many of the process descriptions of ELM have been changed entirely or in part because of the annual character of the vegetation being simulated here.

The general objective of the modeling effort was to simulate seasonal dynamics of biomass in a representative annual grassland ecosystem. To be useful, the model should respond realistically to the wide range of environmental conditions and to common management practices in the annual grassland. Thus, the following specific objectives were considered.

1. To assess the effect on primary production of the following alterations of model conditions:
   a. Variations in weather or in irrigation.
   b. Addition of fertilizers.
   c. Variations in the level or types of herbivorous consumers.
   d. Seeding of leguminous species.
2. To assess the effect of these alterations on:
   a. Carrying capacity.
   b. Botanical composition.
   c. Seed ecology of the plants.
3. To compare primary production and grazing practices (e.g., plant production under various intensities of grazing) among different annual grassland sites.
4. To compare simulation results with field data from annual grassland sites and, if inconsistencies exist, to determine possible reasons for them.

Implicit goals included use of the model to facilitate the organization of diverse information on the annual grassland, to test hypotheses concerning poorly-understood biological phenomena, and to suggest future research directions.

The model is deterministic, it is written in difference equations, and it has been coded in SIMCOMP (Gustafson, 1978), a FORTRAN-like simulation language designed for use in compartment/flow models (Forrester, 1968; Brennan et al., 1970).

Daily flows of carbon, rather than biomass, through the total ecosystem are simulated because carbon is conserved. Flows among compartments or "state variables" of the ecosystem (see Fig. 1, 2, 6, 7, 8, and 9) may indicate the physical movement of material from one place to another (e.g., the fall of standing-dead plants to the litter compartment) or the transformation or reclassification of stationary matter (e.g., the flow between the live-shoot and standing-dead compartments upon death of the plants). The complete cycle of C is simulated, from the atmosphere to producers, then to consumers and decomposers, and finally back to the atmosphere. Flows of N (nitrogen) and P

[1]Accepted for publication October 1, 1982

(phosphorus) are simulated in the nutrient submodels. Temperature, water, and radiation factors are simulated in the weather submodel. Nutrient and weather variables interact with other components of the total system, thus regulating carbon flows. For example, nutrient concentrations of plant shoots regulate the rate of photosynthetic carbon fixation, and soil temperatures regulate the rate of root elongation.

Driving variables for the model, supplied as input data, are daily maximum and minimum air temperatures, precipitation, soil temperature at 105 cm, relative humidity, wind speed, and cloud cover.

The model is essentially one-dimensional, since spatial distinctions among its components are treated only along the vertical axis. State variables for live and dead plant shoots are divided into three height strata. Separate root state variables exist in six soil layers. Variables for soil nutrients, abiotic factors, decomposers, and below ground litter are organized according to soil depth.

Data from the San Joaquin Experimental Range, eastern Fresno County, were used in developing the simulation. However, the model is considered generally applicable to any annual grassland with Mediterranean-type climate through relatively simple changes in site-specific parameters.

Because growth of the annual range begins in fall after sufficient rain to initiate germination has fallen, September 1 was chosen as the starting date of each simulation. Data from 1973–1974 were used in model development. Although the simulation of multi-year periods must be a goal of future modeling efforts, poorly understood year-to-year variability in annual grasslands has prevented useful multi-year simulation.

Necessary input data and model equations describing ecosystem processes were derived as much as possible from field and laboratory data and from the literature. In describing the flows of C through the total ecosystem, it was necessary to include some processes about which little information exists (e.g., the seasonal intake of standing live and dead plant material by herbivores). Model mechanisms describing these processes are based largely on untested hypotheses which appear consistent with observations.

In an attempt to model the complexities of an ecosystem, some simplification is inevitable. This model is considered "all encompassing" since weather, primary producers, consumers, decomposers, and nutrient factors are included; however, some components of these categories or submodels were not included. Only four mammalian consumers were simulated. Other mammals, birds, insects, reptiles, and a host of other consumers were not considered. Decomposers were modeled as if they consisted entirely of microorganisms. Invertebrate soil organisms were not included. Nitrogen and phosphorus were the only nutrients considered, though the importance of sulfur deficiency in California rangeland has been noted (Martin, 1958) and should be considered in future modeling efforts. Finally, though total primary production is simulated, modeling of large numbers of plant species was simplified by grouping producers into five functional categories.

Field data have been used to evaluate performance of the model. Adjustments of parameters and equations of the model have been made with the goal of achieving correspondence of simulated output with field data; however, when output from a simulated system which excludes some major components corresponds with data from the real system, the simulation must be assumed to compensate in some fashion for absence of the excluded factors (Hunt, 1976). For example, biomass which would have been consumed by excluded invertebrates is apparently accounted for in the model by an overestimate of plant respiration, death rates of plants, or decomposition rates, or by an underestimate of primary productivity. A precise explanation of the compensatory

mechanisms is not possible. Despite this consideration, the simulation is useful. A wide variety of system interactions which would be difficult if not impossible to observe in the field may be studied through the use of the model. Comparison of the relative responses of model variables is also possible, particularly those describing primary producers under various environmental conditions and management strategies. Many such comparisons can be made in a short time through simple changes of driving variables or input parameters.

A description of each of the ELMAGE submodels follows. The producer submodel of ELM has been changed substantially for this annual-range application; therefore, a rather detailed description of it is included. Necessary alterations of the nutrient submodels of ELM are also described, including addition of state variables for seeds and separation of legume and nonlegume producer variables (all producers are aggregated in the original nutrient submodels). Few changes have been made in the structure of other ELM submodels (weather, decomposition, and consumer); their use in simulation of the annual grassland is possible through changes in input parameters. Only brief descriptions of these sections of the model are provided. For more information on these submodels and documentation of the total ELM model, see Innis (1978).

WEATHER SUBMODEL

Daily weather observations are used in the weather submodel to simulate the soil and plant-canopy weather parameters influencing the annual grassland ecosystem. This submodel, with a few structural changes described below, is the same as that of the ELM model (Parton, 1978) and consists of a water-flow section and a section describing temperature and solar radiation. Interception of rainfall, infiltration of water into the soil, soil-water drainage, and evapotranspiration of water from the plant canopy and the soil layers are the physical processes simulated in the water-flow section of this submodel (Fig. 1). Interception of rainfall by the standing crop (producer variables are aggregated in the weather submodel) and surface litter is simulated with equations developed for grasses and litter in the annual grassland (Corbet and Crouse, 1968). Rainfall not intercepted is infiltrated into the top soil layer. If water content of the top layer is greater than field capacity, the excess flows into the second soil layer (fast drainage), etc. until there is insufficient water to bring the next lower layer up to field capacity. When the water content of a soil layer is $\leq$ field capacity (slow drainage condition), water drainage from each soil layer is simulated as a function of the water content of each layer using an equation developed by Black et al. (1969) as modified by Parton (1978).

The potential evapotranspiration rate (PE) is calculated using Penman's (1948) equation; it is a function of average daily air temperature, relative humidity, cloud cover, and wind speed. Water intercepted by the standing crop and litter is evaporated at the potential evapotranspiration rate. If total intercepted water is less than daily water loss estimated by PE, then water is removed from the soil layers.

Water is lost from the soil layers through bare-soil evaporation and transpiration. Bare-soil evaporation is assumed to occur in the top three soil layers, 10 cm in depth (this may vary with soil type, from 2 to 15 cm (Lemon, 1956)); it decreases rapidly as those layers become dry. Bare-soil evaporation from each of the top three layers is a function of PE, soil-water content of each layer, average soil-water potential in the top

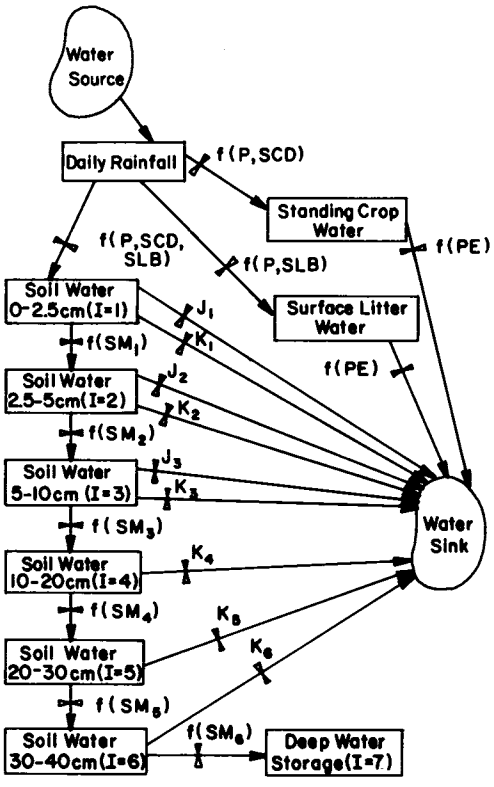

Fig. 1. Flow diagram of water-flow section of the abiotic submodel (modified from Parton, 1978).

P = daily rainfall.
SCD = biomass of the standing crop.
SLB = biomass of the surface litter.
PE = potential evapotranspiration rate.
SM_i = water content of the i^{th} soil layer.

J_i = bare soil evaporation from the i^{th} soil layer: f(PE, SM_i, SCD, weighted average soil water tension in the upper 10 cm of soil, and the biomass of live plant shoots).

K_i = transpiration from the i^{th} soil layer: f(PE, SM_i, weighted average soil water tension in the upper 40 cm of soil, biomass of live plant shoots, and the water absorption coefficient for the live roots in the i^{th} soil layer).

three soil layers (weighted by a water-loss coefficient for each layer, the assumed fraction of bare-soil evaporation coming from each layer), the biomass of live shoots, and the biomass of the standing crop. Transpiration water loss from each soil layer is a function of PE, soil-water content of each layer, average soil-water potential of the soil (weighted by the water-absorption coefficient for the live roots in each soil layer), the biomass of live shoots, and the water-absorption coefficient for the live roots in each layer (Parton, 1978). The water-absorption coefficient for each layer is equivalent to the fraction of total live roots in that layer. These coefficients are recalculated at each time step based on root-distribution information generated in the producer submodel. Finally, deposition of dew has been formulated by Parton (1978) based on equations by Hess (1959).

Temperatures in the plant canopy and the soil are simulated in the heat flow section of the submodel. Average daily temperature at the top of the soil is predicted as a function of the average daily air temperature at 2 m (average of daily maximum and minimum temperatures), PE, biomass of the standing crop, and ratio of the actual evapotranspiration rate to PE (Parton, 1978). Average daily temperature at the bottom of the soil profile of the model is interpolated from monthly mean temperatures at the lowest point in the profile (data input values), and the model simulates soil temperatures at 15 cm intervals using the one-dimensional Fourier heat conduction equation (Munn, 1966).

Shortwave solar radiation on a clear day is calculated as a function of time of year, latitude, and the transmission coefficient, based on an equation presented by Sellers (1965). The influence of cloud cover and reflectivity of the plant canopy on net shortwave radiation is predicted with an equation by Haurwitz (1941).

Daily maximum canopy air temperature is calculated as a function of daily maximum temperature at 2 m and shortwave solar radiation above the plant canopy. Average canopy temperature during daylight hours is simulated by integrating over a truncated sine wave in which the minimum daily air temperature at 2 m (assumed to be the same as the minimum daily canopy temperature) occurs at sunrise, and the maximum daily canopy air temperature occurs at 2 p.m. (Parton, 1978).

Abiotic variables simulated in this submodel were used throughout the ELMAGE model to influence a variety of biological processes. The only feedback from the rest of the model to the weather submodel is through producer variables, and producer information is aggregated for use in this submodel.

PRODUCER SUBMODEL

The seasonal dynamics of herbaceous species in the annual grasslands of California are simulated in the producer submodel. Total production of an annual grassland site is simulated by representing all species of primary producers as five functional groups (Table 1).

TABLE 1. FUNCTIONAL GROUPS OF PRIMARY PRODUCERS

Functional group	Representative species
Early grasses	*Bromus diandrus* Roth. *Festuca* spp.
Later grasses	*B. mollis* L. Miscellaneous grasses
Early forbs (less legumes)	*Erodium* spp. Miscellaneous forbs
Summer forbs	*Eremocarpus setigerus* (Hook.) Benth. *Holocarpha virgata* Keck Miscellaneous summer annual forbs
Legumes	*Trifolium* spp. Miscellaneous legumes

The representative species listed in Table 1 comprise the dominant species at the San Joaquin Experimental Range; the functional groups should apply to most annual grassland areas in California. The organizational framework of the submodel is based on the producer submodel of ELM (Sauer, 1978); however, most mechanisms in this submodel differ from those in ELM. For example, increase in height of the producers in the canopy, increase in rooting depth, and changes in root distribution of the producers over the season are represented in this submodel though not included in ELM. A more detailed description of germination and seedling establishment was required in ELMAGE because of the annual species.

The focus of this model is the seasonal carbon flow through the ecosystem. Plant development through seven stages (phenophases) is simulated in the phenology section of the producer submodel. This information is used to regulate the biological processes in the carbon cycle. Carbon moves from seeds to the shoot and root systems during

germination. As the plants grow, atmospheric carbon moves to the shoots through photosynthesis and is distributed to shoots, roots, and seeds. Respiration returns plant carbon to the atmosphere. Shoot and root death move carbon to standing-dead and belowground-dead structures, respectively. The fall of standing dead moves carbon to surface litter. Live shoots, standing dead, live roots in six soil layers, and seeds are represented by state variables for each producer group (Fig. 2). The leaves and stems are divided into three height strata: 0–10, 10–20, and 20+ cm.

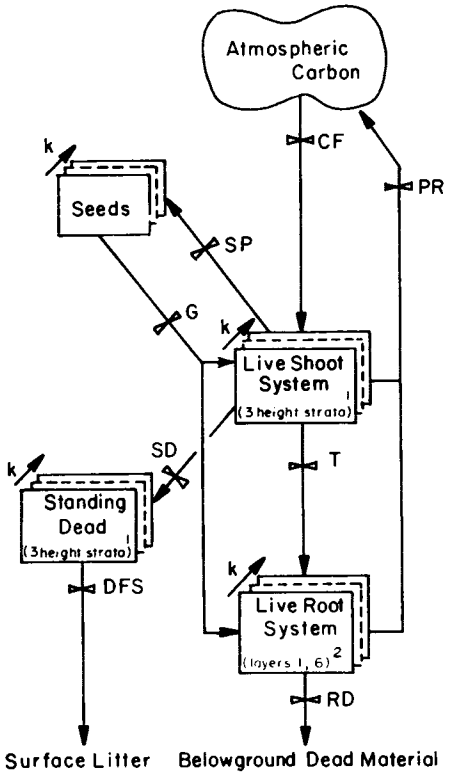

Fig. 2. Carbon flows in the producers.

CF = carbon fixation: f (solar radiation, quantum efficiency, leaf area, plant extinction coefficients, soil water, canopy temperature, shoot nitrogen and phosphorus concentrations, phenology).

PR = plant respiration: f (plant weight, gross photosynthesis, coefficients of maintenance and growth plant respiration).

SP = seed production: f (photosynthesis during the reproductive stage of growth, a rate constant).

G = germination: f (seed weight, soil surface temperature, soil water in upper 5 cm, phenology, a rate constant). Germinating seed carbon is divided into shoot and root fractions. [Onset of germination occurs when a 14-day sum of rainfall exceeds a preset "effective" level (2.5 cm)].

T = translocation from shoots to roots: f (live-shoot weight, live-root weight, shoot nitrogen and phosphorus concentrations, soil water).

SD = shoot death: f (live-shoot weight, phenology, soil water, rate constant).

DFS = standing dead fall to surface litter: f(standing dead weight, rainfall intensity, standing crop water storage, rate constant).

RD = root death: f (live-root weight, phenology, soil water, rate constant).

k = number of producer categories (five in current model application).

1 = live-shoot and standing dead state variables are subdivided into three height strata (0–10 cm, 10–20 cm, 20+ cm).

2 = there are separate root state variables for each producer category in each of the six soil layers.

Phenology

The annual cycle of plants is regulated in the phenology section of the producer submodel by environmental conditions. The stages of growth of primary producers influence other model processes including rates of carbon flow, e.g., daily seed production (carbon flow from shoots to seeds) is influenced by the proportions of each producer in the fruiting stage of growth (Sauer, 1978).

The stages of live-plant development are represented in seven phenological categories (phenophases) (Table 2). Proportions of the live biomass of each producer are distributed through phenophases one to seven. As in nature, the biomass of each producer may exist in more than one phenological state. Distribution of biomass among

stages of growth changes as flows between phenophases simulate phenological progression. The daily rate of flow between two phenophases is a function of an assumed maximum rate of flow between the phenophases, content of the donor phenophase, maximum daily air temperature, net shortwave radiation, and soil-water potential.

TABLE 2. DESCRIPTION OF PRODUCER PHENOPHASES

Phenophase	Stage of growth
1	Seed stage through germination
2	Early vegetative
3	Middle vegetative
4	Late vegetative, initiation of flowering
5	Flowering, beginning fruit development
6	Fruiting (plant may contain buds, flowers, and ripe seeds)
7	Senescence, death

Movement through the phenophases is regulated by a 10-day moving average of the product of daily maximum air temperature and net shortwave solar radiation ($°C \cdot cal \cdot cm^{-2} \cdot day^{-1}$) (Sauer, 1978). Each phenophase is assumed to have a threshold of the temperature-radiation product (TR) before which no outflow occurs and after which flow between phenophases increases linearly with TR to a limit beyond which TR does not influence flow between phenophases. The bounds were established for each of the producer categories by means of data from the San Joaquin Experimental Range. A 10-day moving average of TR is used to simulate delay in the response of plants to changing weather conditions.

The effect of soil-water potential on phenological change is a function of the soil-water potential in each soil layer and the water-absorbing capacity of the roots of each producer in each soil layer. Roots are distributed over six soil layers: 0–2.5, 2.5–5, 5–10, 10–20, 20–30, and 30–40 cm (see "Root Growth"). Water-absorbing capacities are assumed to be proportional to biomass of the live roots of each producer in each soil layer, as in Eq. 1.

DEFINITION OF TERMS USED IN THE PRODUCER SUBMODEL

Term	*Definition*
CDW	Conversion factor from carbon to dry weight ($g\ dry\ weight \cdot g\ C^{-1}$)
CT	Mean daily canopy temperature (°C)
DPP	Standing dead phenology value of a producer (ND)
DR	Diffuse radiation ($cal \cdot cm^{-2} \cdot day^{-1}$)
DSC	Maximum amount of water held in the standing crop during a 1-day period (cm)
DSH	Dead shoot (standing dead) weight ($g\ C \cdot m^{-2}$)

DT	Time step (days)
E_a	Effect of phenology on photosynthesis (ND)
E_n	Effect of shoot concentration of nitrogen on photosynthesis (ND)
E_p	Effect of shoot concentration of phosphorus on photosynthesis (ND)
E_t	Effect of mean photoperiod canopy temperature on photosynthesis (ND)
E_w	Effect of soil-water potential on producer (ND)
EFD	Effect of precipitation on rate of fall of standing dead to litter (ND)
ER_t	Effect of temperature on root elongation (ND)
ERD_p	Effect of phenology on the rate of root death (ND)
ERD_w	Effect of weighted soil-water potential on the rate of root death (ND)
ESD_p	Effect of phenology on the rate of shoot death (ND)
ESD_w	Effect of weighted soil-water potential on the rate of shoot death (ND)
EWC	Effect of water content of the standing crop on the rate of fall of standing dead to litter (ND)
EX	Extinction coefficient of producer (ND)
$\dot{GP}$	Gross photosynthetic rate ($g\ C \cdot m^{-2} \cdot day^{-1}$)
GRM	Growth respiration multiplier (ND)
I_i	Fraction of incident radiation intercepted by standing crop of all producers in height layer i (ND)
K	Rate constant (day^{-1}; value depends on use)
KP	Standing dead phenology constant (ND)
LAI	Leaf area index of producer (m^2 leaf area $\cdot m^{-2}$ ground surface)
LAR	Ratio of leaf area to dry weight of producer ($m^2 \cdot g$ dry weight $^{-1}$)
LDS	Dry weight of live and dead shoots of producer (g dry weight $\cdot m^{-2}$)
$\dot{LI}_i$	Solar radiation that can be intercepted by foliage in height stratum i ($cal \cdot cm^{-2} \cdot day^{-1}$)
LF_i	Fraction of solar radiation intercepted by producer in height stratum i (ND)
$\dot{LS}$	Light saturation level of producer ($cal \cdot cm^{-2} \cdot day^{-1}$)
LSH	Live shoot weight ($g\ C \cdot m^{-2}$)
MP	Parameter which determines rate of mortality increase with density ($m^2 \cdot plant^{-1}$)
$\dot{MRE}$	Maximal rate of root elongation ($cm \cdot day^{-1}$)

MRM	Maintenance respiration multiplier (day^{-1})
MRT	Maximum fraction of daily net photosynthate transferred to producer roots (ND)
$\dot{NDR}$	Nonscattered direct radiation ($cal \cdot cm^{-2} \cdot day^{-1}$)
$\dot{NP}$	Net photosynthate of producer ($g\ C \cdot m^{-2} \cdot day^{-1}$)
P	Daily rainfall (cm water)
PD	Density of producer ($plants \cdot m^{-2}$)
PDW	Producer weight ($g\ C \cdot m^{-2}$)
PH_i	Proportion of producer in phenological stage i (ND)
PPM	Factor controlling daily flows between vegetative phenophases (ND)
$\dot{PR}$	Producer respiration rate ($g\ C \cdot m^{-2} \cdot day^{-1}$)
PW	Permanent wilting point of producer (– bars)
Q	Temporary variable (depends on use)
QE	Quantum efficiency ($moles\ C \cdot Einstein^{-1}$)
R_j	Weight of live roots of producer in soil layer j ($g\ C \cdot m^{-2}$)
$\dot{RDI}$	Daily increase in rooting depth ($cm \cdot day^{-1}$)
RSR	Root-shoot ratio forcing parameter (ND)
RST	Fraction of daily net photosynthate transferred to producer roots (ND)
$\dot{RTD}_j$	Rate of root death in soil layer j ($g\ C \cdot m^{-2} \cdot day^{-1}$)
S	Cumulative product of daily rainfall and mean daily canopy temperature ($°C \cdot cm\ water \cdot day^{-1}$)
SCD	Dry weight of standing crop ($g\ dry\ weight \cdot m^{-2}$)
$\dot{SD}$	Density of seedlings emerging ($plants \cdot m^{-2} \cdot day^{-1}$)
$\dot{SDC}$	Flow of seed carbon to shoots and roots ($g\ C \cdot m^{-2} \cdot day^{-1}$)
$\dot{SDL}$	Flow of standing-dead carbon to litter ($g\ C \cdot m^{-2} \cdot day^{-1}$)
SDR	Scattered direct radiation ($cal \cdot cm^{-2} \cdot day^{-1}$)
SDW	Seed carbon weight ($g\ C \cdot m^{-2}$)
$\dot{SGS}$	Shoot fraction of germinating seeds ($g\ C \cdot m^{-2} \cdot day^{-1}$)
SGT	Minimum soil temperature for seed germination (°C)
SMM	The maximum less the minimum soil temperature for seed germination (°C)
SMW	Mean dry weight of a producer's seed ($g\ dry\ weight \cdot seed^{-1}$)

$\dot{SSA}$	Carbon weight of summer annual shoots if cover were complete (g C · m^{-2})
$\dot{SSD}$	Flow of shoot carbon from dying seedlings (g C · m^{-2} · day^{-1})
$\dot{SST}$	Flow of carbon from shoots to seeds (g C · m^{-2} · day^{-1})
SSW	Carbon weight of live shoots of summer annual plants (g C · m^{-2})
ST	Soil surface temperature (°C)
$\dot{STD}$	Rate of shoot death (g C · m^{-2} · day^{-1})
TR	Ten-day moving average of the product of daily maximum air temperature and net shortwave radiation (°C · cal · cm^{-2} · day^{-1})
WC_j	Water absorbing capacity of producer in soil layer j (ND)
Y	Y-intercept of exponential equation for seedling mortality (ND)
Ψ_j	Soil-water potential of soil layer j (– bars)

$$WC_j = R_j / \sum_{j=1}^{6} R_j \tag{1}$$

In equation 1 and most subsequent equations, parameters and variables that describe plant characteristics are specific to the functional groups of the model. A subscript, k, indicating this specificity is omitted in most cases.

Equation 2 describes the calculation of the effect of soil-water potential on each producer.

$$Q_j = \begin{cases} 1 - \psi_j / PW, & \psi > PW \\ 0 \quad , & \psi \leq PW \end{cases}$$
$$E_w = \sum_{j=1}^{6} Q_j \cdot WC_j \tag{2}$$

Thus, as all soil layers approach field capacity, E_w approaches 1.0; if all soil strata are at or below the permanent wilting point for a producer, E_w is 0.0.

Vegetative, reproductive, and senescent phenology. Vegetative phenological progression is assumed to occur most rapidly at medium water stress and to tail off on either side as a sine function (Eq. 3).

$$PPM = 0.5 \, [\text{sine} \, (\pi \cdot E_w) + 1] \tag{3}$$

PPM is the factor used to reduce the daily flow between vegetative phenophases and is scaled between 0.5 and 1.0. When $E_w = 0.5$ (medium soil-water stress), PPM = 1.0 and there is no reduction of flow rates. As soil-water potential approaches either the permanent wilting point ($E_w = 0.0$) or field capacity ($E_w = 1.0$), PPM approaches 0.5, reducing the daily flow between vegetative phenophases by 50 percent. It is assumed that drought reduces carbohydrate accumulation which decreases phenological change. Abundant soil water also slows progression through vegetative phenophases. Under low water stress, vegetative plants are assumed to accumulate as much carbohydrate as possible and maximize the potential for seed production (Sauer, 1978).

The proportions of each producer which enter the reproductive state and the time spent in the flowering and fruiting phenophases increase with decreasing soil-water stress. Flows from a vegetative to a reproductive state (phenophase 4 to 5) are directly proportional to E_w. At field capacity, there is no reduction of the daily flow to the flowering phenophase. When soil-water potential is at or below the permanent wilting point, there is no flow to the flowering phenophase. Thus, abundant soil water results in faster movement from the final vegetative phenophase to the flowering phenophase.

Drought is assumed to increase flows to the senescent phenophase. Flows from the late vegetative phenophase to senescence (4 to 7) and from fruiting to senescence (6 to 7) are directly proportional to $1.0 - E_w$. Thus, at field capacity, flows to senescence are zero. At the permanent wilting point, flows to senescence reach the maximum. As soil-water stress decreases (E_w increases from 0.0 to 1.0), a decreasing fraction of late vegetative phenophase (4) flows to senescence (7) and an increasing fraction is directed through the reproductive phenophases (5 and 6). Decreases in soil-water stress, then, result in delayed senescence and greater time in the flowering and fruiting phenophases, with a concomitant increase in potential for seed production.

Flows from the flowering to the fruiting phenophase (5 to 6) are assumed to be unaffected by soil-water status under normal to drought conditions; the flows are regulated by a rate constant, the TR level, and the content of the donor phenophase (5). However, if the soil is at or near field capacity ($E_w \geq 0.8$), the flows are from fruiting to flowering. These reverse flows are regulated by a rate constant and the content of the donor phenophase (6).

After a producer enters the reproductive state, it is assumed that some plants in that producer category will continue flowering as long as the soil remains at or near field capacity. Plants of some species which are near maturity may resume flowering with an increase in soil water.

Because producer species are grouped into functional categories, and because day and night temperatures are not distinguished, a detailed simulation of photoperiod and temperature requirements for flowering is not attempted in this model.

Standing dead phenology. To reflect the decrease in palatability and nutritive quality of standing dead plants over time, a rudimentary measure of the status of standing dead was included in the model. This measure was termed "standing-dead phenology"; it is used solely to supply information to the consumer submodel. The decrease in quality of standing dead caused by leaching and microbial activity is assumed to be influenced by rainfall and mean canopy temperature. As the daily product of these factors increases to a preset level, the value of standing-dead phenology increases from seven to nine (an extension of live-plant phenophases), reflecting the change from a recently dead condition to leached and weathered material (Eq. 4).

$$S_{T+DT} = S_T + (P \cdot CT \cdot DT)$$

$$DPP = \begin{cases} (KP \cdot S_{T+DT}) + 7 & , \quad DPP \leq 9 \\ 9 & , \quad DPP > 9 \end{cases} \tag{4}$$

If the mean temperature falls below 0 °C, CT is set equal to 0 °C to avoid a decrease in the cumulative S_{T+DT}. T is time in days and seven and nine are the lower and upper bounds, respectively, of the value of the standing-dead phenology, DPP.

Seed germination

The timing and rates of germination and seedling establishment of annual species are important determinants of the botanical composition of the annual grassland. Studies have indicated that the relative proportions of species which survive the period of germination and establishment are likely to persist throughout the growing season (Heady, 1958; Bartolome, 1976).

Germination in the annual grasslands begins after precipitation has ended the summer drought. It is generally felt that 1.27 to 2.54 cm (0.5 to 1 inch) of rain is sufficient to initiate germination (Bentley and Talbot, 1951; Heady, 1958). The timing of drought-breaking rainfall is variable, and substantial rainfall usually occurs sometime between September and early December. The break of season is specified in the model by computing daily the cumulative rainfall for preceding 14-day periods from 1 September until an "effective" level of rainfall of 2.5 cm is reached (Smith and Williams, 1973).

To simulate the delay between the initiation of germination and emergence, 5 days must elapse following the occurrence of effective rainfall before flows from seeds to shoots and roots can begin. At the time these flows begin, roots are presumed to have been growing for 5 days (Asher and Ozanne, 1966; McCown and Williams, 1968). Therefore, the root fraction of germinating seeds can flow to a soil depth equivalent to the expected depth of penetration of the radicle of each producer between the time of germination and emergence.

Summer forbs are subjected to an arbitrary daylength control, and germination does not begin until a variable which calculates daylight hours reaches a value corresponding to mid-December.

Following the break of season, germination is a function of seed weight, phenology, surface soil temperature, and soil water potential. Germination can occur in the model only if the average soil water potential of the top two layers of soil (5 cm) is greater than -12 bars (Young et al., 1970). No germination can occur during or following the flowering and fruiting stages of growth (phenophases 5 and 6), thus preventing any germination of seeds produced in the current model-year (Laude, 1956).

Precise determinations of soil seed reserves are difficult to make, but it is well known that seed can remain viable in the soil for years (Bartolome, 1976). A parameter, currently 5 percent, insures that a fraction of the seed carbon of each producer which is present at the beginning of each model year remains in the soil after germination has concluded.

If the conditions described above favor germination, rate of germination ($\dot{SDC}$) is a function of seed weight and soil surface temperature as in Eq. 5.

$$\dot{SDC} = SDW \cdot K \cdot [.5 + (.5 \sin[2\pi \cdot (ST - SGT - [.25 \cdot SMM])/SMM])] \quad (5)$$

Thus, a truncated sine function describes the relationship between soil temperature and germination rate shown in Fig. 3 (Young et al., 1973). One-half of germinating seed carbon is translocated to the shoot system and the remaining half to the root system of each producer.

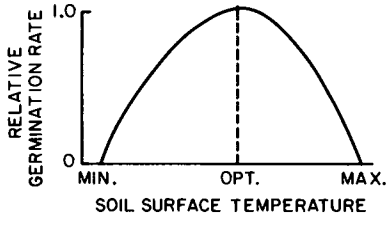

Fig. 3. Relationship between soil surface temperature and seed germination rate.

Seedling mortality

Death of annual plants during the period of germination and establishment represents a substantial proportion of the total mortality of individuals during the season of growth. Approximately one-half of the seedlings in dense stands of annual plants die before reaching maturity (Bartolome, 1976; Biswell and Graham, 1956), and most of this loss of individuals takes place during germination and early growth (Bartolome, 1976).

The density of plants which have emerged previously has been called the most important factor influencing the future of an emerging seedling (Ross and Harper, 1972). Seedling mortality is incorporated in the model as a function of plant density and the weight of germinating seed at each time step. All seedling mortality is assumed to occur at the time of germination. Mortality increases exponentially with increasing density of established plants as in Eq. 6 (Fig. 4).

$$\dot{SSD} = \dot{SGS} \cdot Y \cdot \exp(MP \cdot PD) \quad (6)$$

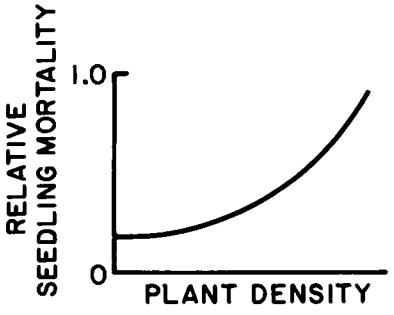

Fig. 4. Relationship between plant density and seedling mortality.

Equation 6 is also used to describe seedling-root mortality, with root death a function of the root fraction of germinating seeds.

The mortality curves differ among the five functional groups of producers with grasses exhibiting a relatively high level of mortality even at low density. All grass seedlings can be expected to die upon germination when grasses have maximum density. There is little mortality of forb seedlings at low density, and no more than one-half of newly emerged forb seedlings die even when the density of established plants is high. The general nature of these relationships was derived from Bartolome (1976); however, mortality data are extremely variable and model functions represent no more than approximations of the processes of seedling mortality.

Plant density

Numbers of individual plants are computed upon germination from the carbon weight of germinating seeds and the average weight of each seed, as in Eq. 7.

$$\dot{SD} = \dot{SDC} \cdot CDW/SMM \quad (7)$$

Existing density of each producer is incremented by $\dot{SD}$ with each day's emergence of seedlings.

Live shoots of summer forb species are typically present at the beginning of a model run on 1 September. Density of these species prior to germination of the current year is a

function of shoot weight per area, estimated weight per area with total cover, and assumed density with total cover (5,000 plants · m^{-2}) as in Eq. 8.

$$PD = 5{,}000\ (SSW/SSA) \tag{8}$$

Plant density is reduced at each time step by mortality of seedlings and of established plants. Since seedling mortality is assumed to occur at the time of germination, the number of seedlings which die each day is determined by dividing the weight of dying seedlings by the average weight of a seed of each producer. Reduction in numbers of established plants is simply formulated as the proportion (by weight) of established plants which die at each time step multiplied by the existing density (i.e., dying plants are of mean weight). We assume the smallest, weakest competitors among established plants die. Their weight plus the weight of dying leaves of surviving plants divided by plant density is assumed to be approximately the mean weight of established plants.

Plant height

Small differences in height among plants allow taller plants a competitive advantage for light, and differences in height early in the season can become more pronounced as the season progresses (Black, 1958; Williams, 1963; Williams et al., 1968). To account for the influence of height on competitive relations, plant height is simulated as a linear function of individual plant weight and the density of each producer. Such linear increases in height per individual plant with increasing density were discerned in data on the growth of *Trifolium subterraneum* (Stern, 1965) and *Bromus mollis* (McCown and Williams, 1968). Since the maximum height, not the mean height, of each producer is to be simulated, mean weight per individual is increased by 30 percent (an estimate of the difference between mean and maximum weight) in the calculation of height in an attempt to represent the tallest plants of each producer. No data that allow simulation of density effects of other producers on the height of a particular producer are available.

Vertical distribution of leaf area

A parameter specific to each functional group of producers is used to convert dry weight of each shoot system to leaf area as in Eq. 9.

$$LAI = LDS \cdot LAR \tag{9}$$

LAR values for grasses decrease over the growing season and are calculated by a quadratic expression developed from data on ryegrass by Fulwood and Puckridge (1970). LAR for the other functional groups is constant.

Three height classes (strata) are used to represent the vertical distribution of leaf area: layer 1 = >20 cm; layer 2 = 10–20 cm; and layer 3 = 0–10 cm. Leaf area is distributed into one or more of these strata depending on the height of each producer. The distribution of leaf area of legumes and some other forbs is likely skewed toward the upper end of their height, at least in part due to senescence of older leaves near the ground (Black, 1958; Stern and Donald, 1962). Grass leaf area is greater in the lower portion of their vertical distribution (Crafts, 1938; Heady, 1950). Weighting factors based on these differences in proportions are used to allocate total leaf area of each producer to the height classes.

Photosynthesis

The process through which carbon compounds are derived from photosynthesis is central to the producer submodel. The general form of the photosynthetic equation using the "law of the minimum" is from Sauer (1978). Functions in the equation are general since functional groups of producers, not species, are modeled, and since the time step of the model is 1 day. The factors influencing photosynthesis are depicted in Eq. 10.

$$\dot{GP} = 1.0368 \cdot QE \cdot \min(E_w, E_t, E_n, E_p, E_a) \cdot \left[\sum_{i=1}^{3} \min(LI_i, LS) \cdot LF_i\right] \quad (10)$$

The relationship between light quanta and calories of incident solar radiation has been estimated to be 8.6μ Einstein · cal^{-1} (Loomis and Williams, 1963). This estimate is used to derive the constant, 1.0368, which converts cal · cm^{-2} to g C · m^{-2}.

The effect of soil-water potential on photosynthesis (0 to 1) is linear between the permanent wilting point and field capacity. Although photosynthetic rates are controlled actually by plant-water stress and only indirectly by soil-water stress (Kramer, 1969), rates of photosynthesis have been shown to be closely related to soil-water stress in plants as diverse as tomatoes and pine trees (Brix, 1962).

Average canopy air temperature during the daylight hours is simulated in the weather submodel by integrating over a truncated sine wave in which the minimum daily air temperature is assumed to occur at 0600 hours and the maximum air temperature at 1400 hours. Research has suggested a generally similar response of photosynthesis of plants of temperature climates to changes in air temperature (Connor et al., 1974; Mooney et al., 1964). Model values for temperature minima, optima, and maxima differ slightly for the functional groups of producers, but the general relationship between average canopy temperature and gross photosynthesis, derived from literature, is shown in Figure 5.

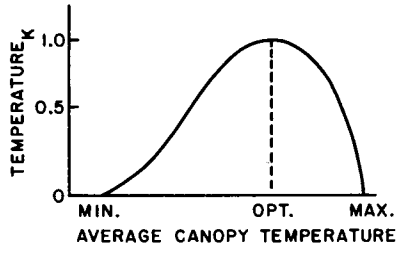

Fig. 5. Relationship between average photoperiod canopy temperature and effect of temperature on photosynthetic rate.

Effect of shoot nitrogen and phosphorus. Seligman et al. (1975) suggested that there is a plant nitrogen concentration above which increases in nitrogen do not increase photosynthesis and that, as a plant matures and accumulates carbohydrates, the nitrogen concentration of the plant and the minimum concentration for an unrestricted growth rate decrease. They further indicated that minimum nitrogen concentration for unrestricted growth of grasses changes from 2.0 percent to 2.5 percent during the early vegetative stage of growth to around 1.0 percent for later stages of maturity. Reuss and Innis (1977) implement the same concept with different limiting values.

Separate linear relationships are used in the model to describe the effect of shoot nitrogen concentration on photosynthesis for legumes and nonlegumes when the mean

growth stage of plants is vegetative (mean phenophase ≤ 4) or reproductive. Nitrogen concentrations in the shoots of legumes and in the shoots of aggregated nonlegume producers are simulated in the nutrient submodels. Values for the minimum nitrogen concentrations for photosynthesis (N-starvation level) and for the minimum concentrations for an unrestricted photosynthetic rate were suggested by studies of the nitrogen content of annual plants in various stages of growth (Gordon and Sampson, 1939; Gladstones and Loneragan, 1975; unpublished data from the San Joaquin Experimental Range) and with various levels of nitrogen fertilization (Jones, 1963). As the shoot concentration of nitrogen varies between these levels, the nitrogen control on phytosynthesis, E_n, varies linearly from 0 to 1.

TABLE 3. SHOOT NITROGEN CONCENTRATION (%) CONTROLS ON PHOTOSYNTHESIS

Item	Nonlegumes		Legumes	
	Vegetative	Reproductive	Vegetative	Reproductive
N-starvation level ($E_n = 0$)	0.6	0.5	0.8	0.6
Minimum for unrestricted photosynthesis ($E_n = 1$)	2	1	3	2.5

Shoot phosphorus required for maximum yield decreases from the early vegetative stage to the flowering stage of growth in all annual range species that have been studied (Ozanne et al., 1969; Jones et al. 1972). Linear relationships between photosynthesis and shoot P concentration are used in the same way as for nitrogen.

TABLE 4. SHOOT PHOSPHORUS CONCENTRATION (%) CONTROLS ON PHOTOSYNTHESIS

Item	Nonlegumes		Legumes	
	Vegetative	Reproductive	Vegetative	Reproductive
P-starvation level ($E_p = 0$)	0.1	0.05	0.1	0.05
Minimum for unrestricted photosynthesis ($E_p = 1$)	0.85	0.12	0.75	0.15

Phenology. Photosynthesis is not affected by producer phenology until flowering (mean phenophase = 5) when the effect of phenology on photosynthesis begins decreasing linearly from one and becomes zero at senescence (mean phenophase = 7). Whole-plant photosynthetic rates have been shown to begin decreasing at the time of flowering in wheat and other annual species (Singh and Lal, 1935).

Insolation. Daily values of diffuse and direct photosynthetically active radiation ($cal \cdot cm^{-2} \cdot day^{-1}$) are simulated in the weather submodel as functions of time of year, latitude, transmission coefficient, reflectivity of the plant canopy, and average daily cloud cover. A portion of direct radiation is scattered as it passes through the plant canopy. A scattering coefficient of 0.25, constant throughout the year, is used in this model (i.e., 25 percent of direct radiation is scattered). One-half of the scattered component of direct radiation is assumed unavailable for photosynthesis, either because of absorption at the soil surface or because it escapes upward through the canopy. The other half is assumed to arrive at plant surfaces from all directions (de Wit, 1965), and therefore can be absorbed. All unscattered direct radiation ($[1 - 0.25] \cdot$ direct radiation) can be intercepted by the shoot systems of the plants. Equation 11 describes the amount of photosynthetically active radiation which can be intercepted by plant shoots in the top layer of the plant canopy (LI_1 in $cal \cdot cm^{-2} \cdot day^{-1}$).

$$\dot{LI}_1 = \dot{DR} + \dot{NDR} + (0.5 \cdot \dot{SDR}) \quad (11)$$

The interception of radiant energy for use in photosynthesis is dependent upon the leaf area in each of the height layers, the extinction coefficient of each of the producers, and the proportion of live shoots in the standing crop. The calculation of the fraction of incident radiation intercepted by all producers in layer 1 is based on a modified form of the Bougeur-Lambert function:

$$Q_1 = \sum_{k=1}^{5} (EX_k \cdot LAI_{k,1}) \quad (12)$$

$$I_1 = 1 - \exp(-Q_1) \quad (13)$$

The proportion of radiation intercepted by the live (photosynthetically active) shoots of producer k in layer 1 ($LF_{k,1}$) is calculated as:

$$LF_{k,1} = I_1(LAI_{k,1} / \sum_{k=1}^{5} LAI_{k,1}) \cdot (LSH_k / [LSH_k + DSH_k]) \quad (14)$$

Incident radiation which is intercepted in height layer 1 cannot be intercepted in lower layers in the canopy. The intensity of radiation at height layer 2 ($\dot{LI}_2$ in cal · cm^{-2} · day^{-1}) is

$$\dot{LI}_2 = \dot{LI}_1 - (\dot{LI}_1 \cdot I_1)$$

Obviously, if there is no leaf area in height layer 1, there can be no interception there and $\dot{LI}_2 = \dot{LI}_1$. The fraction of radiation intercepted by the live shoots of each of the producers in the lower layers of the canopy and the intensity of radiation at the bottom layer of the canopy are calculated in a similar fashion.

A light saturation level ($\dot{LS}$) is assumed to occur for the producers in the model. Since solar radiation is calculated on a daily basis, $\dot{LS}$ is expressed as a daily total of radiation. When the intensity of radiation exceeds $\dot{LS}$, radiation during the midday period of greatest irradiance is assumed to be sufficiently high to saturate the canopy. At that point, $\dot{LS}$ is used in the calculation of the photosynthetic rate. Only the top layer of the canopy is likely to be affected by the light-saturation level because of the attenuation of radiation as light passes through the canopy.

The moles of light quanta (Einsteins) required to reduce a mole of carbon dioxide to carbohydrates through the photosynthetic process is known as the "quantum requirement." In a study of tropical pasture plants, quantum efficiency (moles CO_2/Einstein) was calculated to be 0.1 for the C_4 species and 0.06 for the C_3 species (Ludlow and Wilson, 1971). A value of 0.09 is used to represent quantum efficiency in the model.

Respiration and net photosynthesis

Total respiration may be viewed as the sum of a growth fraction, which is involved in the synthesis of new tissue, and a maintenance fraction, necessary for the maintenance metabolism of extant plant tissue. On the basis of work with white clover plants, McCree (1970) has suggested that the maintenance fraction of respiration is related to plant dry weight and the growth fraction of respiration is a function of photosynthetic rates. McCree's (1970) model is the basis for the respiration function shown in Eq. 15.

$$\dot{PR} = (\dot{GP} \cdot GRM) \cdot (PDW \cdot MRM) \tag{15}$$

The constants GRM (dimensionless) and MRM (day^{-1}) reflect the relative contributions of growth and maintenance respiration, respectively, to the total respiration of a producer. Model estimates of their respective values are 0.25 and 0.01.

The net photosynthetic rate of each producer is the difference between the gross photosynthetic rate and the plant respiration rate at each time step.

Root growth

Partitioning. The interdependence of root and shoot growth has been characterized as a functional equilibrium by Brouwer and de Wit (1969). They found that when either roots or shoots of growing bean plants were partially excised, the growth rate of the undisturbed plant organs was reduced and the original root:shoot ratio was rapidly restored. The translocation of daily net photosynthate from shoots to roots in the model is based on the assumption that, in the absence of environmental stress, root:shoot ratios remain relatively constant for each functional group of producers. Root:shoot ratios derived from estimates of above and belowground components of mixed annual pasture at the San Joaquin Experimental Range ranged from 0.64[1] to 0.72[2]. Studies of annual plants, including several of the species simulated, have shown greater root:shoot ratios for grasses than for forbs (Stern, 1965; Asher and Ozanne, 1966; Gerakis et al., 1975). The calculation of the root-fraction of daily net photosynthate (RST) is shown in Eq. 16.

$$\begin{aligned} Q &= RSR \cdot \left(LSH / \sum_{j=1}^{6} R_j\right) \\ RST &= \begin{cases} Q & , \quad Q < MRT \\ MRT & , \quad Q \geq MRT \end{cases} \end{aligned} \tag{16}$$

MRT, the maximum fraction of net photosynthate which can be translocated to the roots of a producer per day, varies from 0.38 for winter annual forbs to 0.68 for grasses. If net photosynthesis is zero, translocation from shoots to roots is zero.

A diminished supply of nitrogen is known to increase the root:shoot ratio of plants (Brouwer, 1966). Decreased phosphorus was shown to increase root:shoot ratios in ryegrass and white clover when soil water and nitrogen were not limiting (Davidson, 1969). Shoot concentrations of N and P in the model are assumed to reflect relative availability of these nutrients. When stress due to low concentration of nitrogen or phosphorus becomes severe (E_n or $E_p < 0.1$), the flow of net photosynthate from shoots to roots increases to the maximum (MRT).

Decreasing availability of soil water increases the root:shoot ratios of plants, including grasses (Brouwer, 1966; Peters and Runkles, 1967; Black, 1968; Davidson, 1968). Thus, when soil water approaches the permanent wilting point of the producers in the model ($E_w < 0.2$), shoot-to-root translocation increases to the maximum (MRT).

Though a reduction in light intensity has been shown to induce decreases in root:shoot ratios (Asher and Ozanne, 1966; Brouwer, 1966), a mechanism for representing this effect was not included.

[1] Woodmansee, R. G., D. A. Duncan, D. C. Coleman, and M K. Campion. Dynamics of roots and soil water in an annual grassland ecosystem. Manuscript in preparation.

[2] Duncan, D. A., and R. G. Woodmansee. Plant biomass, soil water dynamics, and primary production in an annual grassland ecosystem. Manuscript in preparation.

Distribution of roots. Rates of root elongation for each of the functional groups of producers under optimal conditions were derived from work by Asher and Ozanne (1966). Daily increase of rooting depth of each producer after germination is a function of the maximum rate of soil penetration, soil temperature, and soil water. The optimum temperature for root elongation is assumed to be 25 °C in the model (Erickson, 1959; Friend, 1965). Erickson (1959) plotted the rate of elongation versus temperature and the resulting curve, used in this model, was similar to that shown in Fig. 5. The calculation of the daily increase in rooting depth ($\dot{RDI}$ in cm · day^{-1}) is

$$\dot{RDI} = \dot{MRE} \cdot ER_t \tag{17}$$

Black (1968) has indicated that root growth into dry soil is limited. High soil-water stress has been shown to reduce rate of root elongation (Peters and Runkles, 1967). When soil water in the area of root elongation reaches a potential equivalent to 80 percent of the permanent wilting point of each producer in the model, $\dot{RDI}$ becomes zero.

The root fraction of net photosynthate which flows to each of the six soil layers each day (described in the "Phenology" section) is dependent on maximum depth of the roots of each producer (the cumulative sum of RDI), and on the expected proportion of root growth in each of the soil layers which contain roots. The greatest proportion of annual plant roots is found at shallow depths, root biomass decreasing with increasing depth (Bennett and Doss, 1960; McKell et al., 1962). More than 80 percent of the root biomass in 30 cm of soil was found in the top 10 cm in 1974 at the San Joaquin Experimental Range[3]. The modeled root distribution of grasses is more shallow than that of forbs.

A matrix of the proportions of roots of each producer in the soil layers is used to apportion the root fraction of net photosynthate among the soil layers at each time step. For example, if the rooting depth of producer k were 20 cm, photosynthate flowing to roots would be divided among the top four soil layers (0–2.5, 2.5–5, 5–10, and 10–20 cm), with relatively greater proportions of carbon flowing to the upper layers. The matrices used were developed through model testing; their use results in a root distribution at season's end which is similar to the vertical distribution of roots on annual range reported by McKell et al. (1962). Distribution of roots in the soil is a determinant of the absorptive capacities of roots at various depths and thus affects the way plants respond to differences in soil-water potential throughout the soil profile.

Seed production

Survival of the annual species represented in the model is entirely dependent upon seed production. Though viable seeds may remain in the soil for years, seed production during each year is an important determinant of the relative abundance of species the following year (Harper, 1977). Carbon for the production of seeds may come directly from photosynthesis in the shoot system, the fruit, or from previously elaborated photosynthate in the plant (Milthorpe and Moorby, 1974). Thorne (1966) found that most of the carbohydrate in the grain of barley and wheat comes from photosynthetic activity after the ears emerge. Though similar evidence relating to the producers modeled could not be found, it is assumed that production of seeds of these annual species depends on photosynthesis during the reproductive stage of growth, and not on carbohydrate stored in the plant. Equation 18 describes seed production.

$$\dot{SST} = (PH_5 + PH_6) \cdot \dot{NP} \tag{18}$$

[3]Duncan, D. A., and R. G. Woodmansee. Plant biomass, soil water dynamics, and primary production in an annual grassland ecosystem. Manuscript in preparation.

Annual plants typically produce an abundance of seed (Biswell and Graham, 1956). Environmental conditions are known to affect the development of seeds (Ryle, 1965). General estimates of the seed proportion of total production of particular species in a mixed annual stand are difficult to obtain. Rossiter (1966) estimated that seeds made up slightly more than 10 percent of the total production of dry weight in a grazed annual-type pasture. In a study involving subterranean clover grown with barley, the weight of clover seed was 26 to 27 percent of the dry weight of clover shoots at the end of the season (McGowan and Williams, 1971). General estimates of seed production of the species modeled may range between 10 percent and 30 percent of yearly shoot production. Because seed production is simulated as a function of photosynthesis, it is indirectly dependent on the extant leaf area of the producers and on environmental conditions at the time of seed synthesis.

Shoot death

Leaves of plants in a grassland community die throughout the growing season. In a study of leaf death in a ryegrass-white clover pasture, Hunt (1971) observed that losses of herbage due to leaf death through the season may amount to as much as 40 percent of total production, depending on species and season. In one laboratory study, the average life span of a white clover leaf was observed to be only 20 days (McCree, 1970).

At least one cause of leaf death is the progressive shading of lower leaves leading to their senescence as a pasture increases in height (Donald, 1963). Brougham (1958) observed the accelerated senescence of white clover leaves when a LAI of about 4 was reached; he attributed this to the intense shading caused by the dense canopy of leaves. As plants increase in age, they contain an increasing proportion of older, dying leaves, and total shoot death thus increases (Robson, 1973).

A significant decline in numbers of individual plants through the season also has been observed. In one 3-year study at the San Joaquin Experimental Range, about 50 percent of the plants in dense stands of annual plants died each year before reaching maturity (Biswell and Graham, 1956). While much of this mortality apparently occurs during the phase of plant establishment (Bartolome, 1976), the rate of plant death increases at the end of the season as well. High soil-water stress increases the rate of shoot death.

Varying rates of leaf death due to different foliar environments in the canopy are not distinguished, and only the rate of death of the total shoots of each producer category is calculated. Total shoot death (i.e., the flow of live-shoot biomass to the standing-dead category) is a function of shoot weight, phenology, soil-water potential, and rate constants, as shown in Eq. 19.

$$\dot{STD} = LSH \cdot [(K_p \cdot ESD_p) + (K_w \cdot ESD_w)] \tag{19}$$

The effects of soil-water potential (ESD_w) and phenology (ESD_p) are both nondimensional multipliers. Soil water stress can cause shoot death irrespective of the phenological state of a producer. ESD_w increases linearly from 0 to 0.1 as the effect of soil-water potential (E_w) decreases from 0.3 to 0 (permanent wilting point). The effect of phenology increases linearly from 0 to 0.3 and from 0.3 to 1.0 as the mean phenophase of a producer increases from one to four and from four to seven, respectively.

Root death

Fundamental difficulties are encountered in root studies, such as the fragility of roots, the identification of the roots of an individual plant in a community, and even the separation of live from dead roots when the root system of a plant is exhumed. Model root-death functions are necessarily general. Root death is modeled similar to shoot death in that it is a function of root weight, phenology, soil-water potential, and a rate constant. Equation 20 describes the calculation of the rate of root death:

$$\dot{RTD}_j = R_j \cdot K \cdot ERD_p \cdot ERD_w \tag{20}$$

The effects on root death of soil-water potential (ERD_w) and phenology (ERD_p) are also nondimensional multipliers. The effect of phenology is identical to that of the shoot death function. ERD_w is 0.75 except when there is high soil-water stress (i.e., $E_w < 0.1$). As the effect of soil-water potential decreases from 0.1 to 0 (permanent wilting point), ERD_w increases from 0.75 to 1.5. That is, the rate of root death is doubled.

Transfer of standing-dead plant material to surface litter

A grassland community is significantly affected by the presence of standing-dead plants. Standing dead interferes with the interception of light by growing shoots, and rainfall is intercepted by and evaporated from the surfaces of standing-dead material, thus preventing its addition to the soil-water reservoir. It is assumed that the standing dead is knocked down during rainstorms and falls because of a decrease in mechanical strength with an increase in water content (Sauer, 1978). Simulation of this process is based on the hypothesis that the rate of movement of standing dead to litter is a function of rainfall intensity and the water content of standing dead (Eq. 21).

$$EFD = \begin{cases} 0.5P, & 0.0 \leq P \leq 1.0 \\ 0.5, & P > 1.0 \end{cases}$$

$$Q = 2000 \cdot DSC/SCD \tag{21}$$

$$EWC = \begin{cases} 0.5Q, & 0.0 \leq Q \leq 1.0 \\ 0.5, & Q > 1.0 \end{cases}$$

$$SDL = DSH \cdot K_s \cdot (EFD + EWC)$$

The constant, 2000, is based on the assumed maximum water-holding capacity of the standing crop. The rate constant, K_s, may be varied between 0.01 and 0.35 to reflect the relative durability of the stems of a producer.

CONSUMER SUBMODEL

The dynamics of selected annual grassland mammals are represented in the consumer submodel principally to describe the effect of consumers on the annual grassland. Anway (1978) has referred to his consumer submodel of ELM (used with few changes in ELMAGE) as canonical in the mathematical sense. That is, each of the processes describ-

ing consumer dynamics is represented with a single code formulation. Input parameters describe the individual and population characteristics of each consumer species that is simulated.

Consumers affect grassland primarily through food intake and elimination. These processes are influenced by the numbers and biological status of the animals and by the quality and availability of food sources. Metabolic energy requirement, diet selection, food utilization, and biological index are calculated for the mean individual of each population. Each of the consumer characteristics which is simulated is assumed to be normally distributed within each generation of consumer. Natality and mortality are distributed over each population.

The biological index is included as a general measure of the physiological status of each consumer as a function of age and weight. The age index is a function of the animal's relative age (simulated age divided by average life-span). Very young and very old animals have a low age index while the age index of mature consumers approaches 1. The weight index is a function of the deviation of an animal's weight from the expected weight of that consumer (described below). Animals at or near the expected weight have a weight index of 1. As the deviation of an animal's weight from its approximate expected weight increases, the weight index decreases. The biological index influences reproduction, energy balance, diet selection, and other consumer functions (Anway, 1978).

OUTLINE OF MAJOR CONSUMER CALCULATIONS (EACH COMPUTATION IS SPECIFIC TO A CONSUMER CATEGORY* (AFTER ANWAY, 1978))

Food required to meet metabolic energy requirement, $\dot{F}$

$$\dot{F} = 70 \cdot W^{0.75} \cdot HT \cdot AF \cdot CF \cdot DT/EC$$

Diet selection

Preference per food category, FP_i

$$X_i = FQ_i \cdot (1.01 - I_b) \cdot I_p$$

$$FP_i = X_i / \Sigma X_i$$

Intake per food category, $\dot{FI}_i$

$$\dot{FI}_i = ([\dot{F}/D] + \dot{H} + \dot{F}_o) \cdot EC_w \cdot EC_c \cdot EC_a \cdot EC_d \cdot FP_i$$

Secondary production increment, $\dot{SP}$

$$\dot{SP} = \dot{TI} - \dot{FCS} - \dot{GS} - \dot{URN} - \dot{F} - \dot{F}_o$$

Biological index, BI

$$BI = \begin{cases} \min(I_a, I_w) \text{ , if } I_a \leq 0.7 \text{ or } I_w \leq 0.7 \\ (I_a + I_w)/2 \text{ , otherwise} \end{cases}$$

Mortality, $\dot{M}$

$$\dot{M} = \dot{M}_a + \dot{M}_p + \dot{M}_s + \dot{M}_o$$

Average adult weight, W

$$W_{T+DT} = (W_T \cdot N_T + [\dot{SP}/1000.] - [\dot{M} \cdot W_d/RA])/N_{T+DT}$$

Natality, N_o

$$N_o = N_m \cdot FF \cdot N_e \cdot BI$$

Birth weight, W_b

$$W_b = 0.053 \cdot W \cdot BI$$

* These calculations are executed at each time step for each consumer generation; a continuous inventory of intrapopulation dynamics is thus maintained.

DEFINITION OF TERMS USED IN THE CONSUMER SUBMODEL

Symbol	*Definition*
A_s	Age, simulated (days)
AF	Activity factor (ND)
BI	Biological index (ND)
CF	Carbon content of food (g C · g dry weight $^{-1}$)
D	Digestibility (ND)
DT	Time step (days)
EC	Energy content of food (kcal · g dry weight $^{-1}$)
EC_a	Effect of age on consumption (ND)
EC_c	Effect of density on consumption (ND)
EC_d	Effect of digestibility on consumption (ND)
EC_w	Effect of weight deviation on consumption (ND)
$\dot{F}$	Food required to meet metabolic energy requirements (g C · individual $^{-1}$ · day $^{-1}$)
$\dot{F}_o$	Food needs of offspring (g C · individual $^{-1}$ · day $^{-1}$)
FF	Fraction female (ND)
$\dot{FI}_i$	Intake per individual per food category (g C · individual $^{-1}$ · day $^{-1}$)
FP_i	Preference for food of category i (ND)
FQ_i	Quantity of each food category i (g C · m $^{-2}$)
FCS	Feces (g C · individual $^{-1}$ · day $^{-1}$)
GS	Gas (g C · individual $^{-1}$ · day $^{-1}$)
H	Food needs carried forward from previous time step (g C · individual $^{-1}$ · day $^{-1}$)
HT	Heat increment (ND)
I_a	Index of relative age (ND)
I_b	Food biological index (ND)
I_p	Food palatability index (ND)
I_w	Index of relative weight (ND)
LS	Life span (days)
$\dot{M}$	Total mortality (individuals · day $^{-1}$)
M_a	Mortality from old age (individuals · day $^{-1}$)

$\dot{M}_o$	Mortality from other causes (individuals · day $^{-1}$)
$\dot{M}_p$	Mortality from predation (individuals · day $^{-1}$)
$\dot{M}_s$	Mortality from starvation (individuals · day $^{-1}$)
N	Density of animals (individuals · m $^{-2}$)
N_e	Number of offspring expected per mature female (ND)
N_m	Density of mature individuals (individuals · m $^{-2}$)
N_o	Density of offspring (individuals · m $^{-2}$)
RA	Population reference area, established as a function of initial density: 1 / N · 100 (m^2)
$\dot{SP}$	Secondary production increment (g C · m $^{-2}$ · day $^{-1}$)
$\dot{TI}$	Total intake (g C · individual $^{-1}$ · day $^{-1}$)
$\dot{URN}$	Urine (g C · individual $^{-1}$ · day $^{-1}$)
W	Animal weight (kg · individual $^{-1}$)
W_b	Birth weight (kg · individual $^{-1}$)
W_d	Average weight of individuals dying per time step (kg C · individual $^{-1}$)
W_e	Expected weight of an animal (kg · individual $^{-1}$)
W_m	Weight of mature animal (kg · individual $^{-1}$)
X_i	Temporary variable used in calculation of food preference (g C · m $^{-2}$)

Up to six consumer categories are used in the current model application to describe four consumer species: cattle, sheep, deer, and ground squirrels. Two categories may be used for cattle to allow a distinction to be made between replacement heifers and the rest of the simulated herd. Thus, different initial values of model parameters, including age, weight, and number, may be specified for the replacement animals. Similarly, two categories may be used to distinguish replacement ewes from other sheep.

Animal density (stocking rate for livestock) in numbers (fraction) of animals per m^2 is specified for each consumer category through an input parameter. Reproduction of cattle, sheep, and deer occurs on preset dates.

The birth of ground squirrels occurs when an environmental variable (the 10-day moving average of the product of solar radiation and maximum air temperature) reaches a threshold value. The health and maturity of potential parents also affects reproduction. A biological index of 0.83 (on a scale of 0.0 to 1.0; derived through exercise of the model) is necessary for reproduction to occur in each consumer generation.

Up to 15 food categories are made available to each consumer through parameter inputs (Fig. 6). The food biological index referred to in "Outline of major consumer calculations" is calculated for each food category to reflect the quality of the food type.

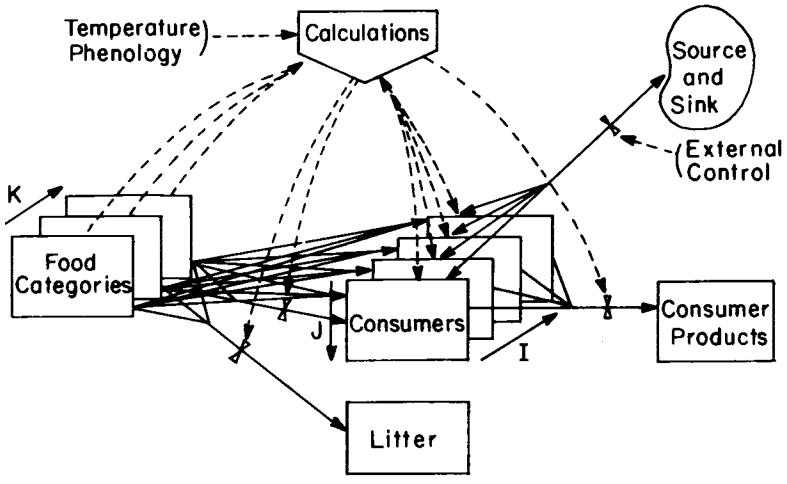

Fig. 6. Flow diagram of mammalian consumer submodel (after Anway, 1978).
Food categories: K = 1, 15; consumer categories: I = 1, 6; consumer age classes: J = 1, 10.
Material flows (carbon) are represented by solid arrows. Information flows are represented by dashed arrows. State variables are represented by boxes.

The food biological index is the phenological index supplied by the producer submodel and converted to a scale of 0.0 to 1.0, increasing with phenological stage. Increased preference of consumers for plant food of low biological index is incorporated in the preference calculations by subtracting the index from 1.01 (the 0.01 insures that the remainder does not become zero). Most of the food sources are simulated in the producer submodel (i.e., live shoots, standing dead, and seeds of the five producer categories). However, other important food sources may be supplied through tabular inputs which vary over time. In this way browse is supplied for all consumers, and insects are provided for ground squirrels.

Consumer products include CO_2, methane, feces, urine, and dead animal biomass. Flows of consumer variables are calculated daily to simulate producer-consumer and consumer-decomposer dynamics. Flows to the model's source and sink primarily represent human manipulation of livestock numbers. The removal of specified numbers of cattle or sheep (to reflect their sale) may be accomplished through "EVENT" subroutines (Gustafson, 1978) which occur on a preset day of a model run.

Given the canonical approach used in this submodel, some general relationships have been used in the simulation of mammalian consumers. For example,

$$W_e = W_m[1 - \exp(-9A_s/LS)] \quad (22)$$

Equation 22 is based on the relationship of life-span, body size, and growth rate proposed by Brody (1945). Simulated age is the age of the consumer cohort (generation) considered in the calculation. The relationship is used in this submodel to influence food intake, rate of mortality, and the biological index previously described. It is also used to predict birth weight. When a birth age of 0.006 · life-span is specified for each consumer, the equation predicts expected weights within 10 percent of observed birth weights (Altman and Dittmer, 1964).

Significant deviation from the expected weight for a consumer can result in "starvation" mortality. If the mean weight of a consumer population deviates from expected weight more than a preset amount for each consumer, starvation mortality (proportional to the population's weight deviation) is calculated.

Another general relationship used in this submodel is the description of an offspring's food dependence period as 0.025 · life-span (Anway, 1978). The proportion of dependence decreases over this period for the herbivores in the model. Using the growth curve previously described (Brody, 1945), this formulation allows offspring to reach approximately 60 percent of adult weight by weaning time under normal conditions. This weaning weight is reasonably comparable to observed data (Altman and Dittmer, 1964; Moen, 1973).

A highly resolute description of animal physiology is not possible with a model composed of such general functions. However, this submodel provides an overview of the dynamics of selected grassland consumers under a variety of conditions. Representation of the interrelationships between selected consumers and other components of the ecosystem is the focus of the ELMAGE application of this model. Of particular importance is the prediction of the impact of various levels of consumer pressure on the primary producers of the model.

DECOMPOSITION SUBMODEL

There are two major obstacles to modeling the processes of decomposition in a grassland ecosystem. (1) Decomposing substrates are heterogeneous and their various components can be expected to decompose at different rates (Floate, 1970). (2) Though huge populations of microbial decomposers may exist in the ecosystem, not all of these organisms are active at any time (e.g., Clark and Paul, 1970). These obstacles are dealt with in this submodel by assuming that (1) complex substrates may be represented simply as consisting of rapidly decomposing and slowly decomposing components; (2) rate of decomposition in the annual grassland is independent of total size of microbial populations; and (3) decomposers exist in either an active or an inactive state, and their activity level is more important for modeling purposes than their taxonomic identity. Decomposers in the model consist entirely of microorganisms and are not distinguished taxonomically.

With one exception, structure of the decomposition submodel of the ELMAGE model is identical to that of ELM (Hunt, 1978). In the ELMAGE decomposition submodel, nonlegume producers are aggregated and legumes are considered separately for flows from live shoots and roots to substrate compartments; in the ELM submodel all producer variables are aggregated.

Substrates and decomposers are divided into four groups according to their position in the soil or on the surface (Fig. 7). Variables simulated in the abiotic and nutrient submodels influence flows in the decomposition submodel. Model code provides for the interface of different submodel depth structures. Inputs to the substrate compartments are from the producer and consumer submodels. Flows of carbon from substrate compartments to decomposers represent decomposition, and respiration is represented by flows to the CO_2 sink from active and inactive decomposers. Flows from decomposers to substrate compartments represent the death of decomposers. Substrate moves from the surface to the upper belowground litter compartments through mechanical transfer, and leaching moves substrate from the labile compartment in each layer to the next lower layer.

Two exponential decay equations are used to predict the daily decomposition rates of labile or rapidly decomposing substrates (e.g., sugars, starches, and proteins), and of resistant or slowly decomposing substrates (e.g., cellulose, lignin, fats, and waxes) under

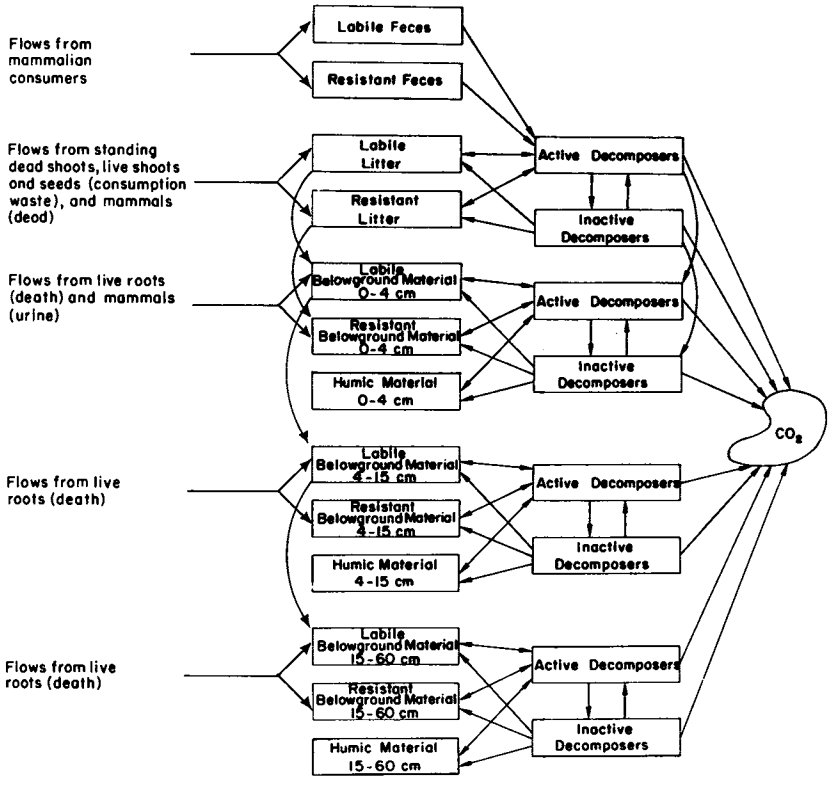

Fig. 7. Flow diagram of the decomposition submodel (modified from Hunt 1978).

constant conditions. The labile and resistant fractions of live shoots and roots which flow to substrate compartments (through death of roots and waste of shoot material by grazing consumers) are predicted from the nitrogen:carbon ratio of the shoots and roots. The proportions of labile and resistant components of other types of producer and consumer biomass (i.e., standing dead, seeds, feces, and dead consumers) are assumed to be constant for each category of material. Temperature and water factors affect decomposition rates of substrates in each decomposition layer. In addition, concentration of inorganic nitrogen in the soil affects the decomposition rate of subsurface substrates.

Felbeck's (1971) theory of humus formation is adopted in this model. Humic materials are assumed to be produced intracellularly by microbes and released on their death. Thus, upon the death of microbes in the model, a small fraction of their biomass (0.003) flows to humic material (Hunt, 1978). Humus decomposes very slowly (Campbell et al., 1967) and at a low, constant rate in the model.

Other processes simulated in the decomposition submodel are leaching and mechanical transfer of biomass. Leaching is represented by flows of labile substrate from surface litter to the upper soil layer, from the upper to the middle layer, and from the middle to the bottom layer. Leaching is a function of temperature and rate of water movement.

In the absence of information on incorporation of particulate material into the soil (by animal activity or water movement), a constant small proportion of surface litter and surface decomposers is transferred to the upper soil layer each day to reflect the assumption that some mechanical transfer occurs (Hunt, 1978).

Decomposers in each of the submodel layers are divided into a metabolically active fraction and an inactive fraction consisting of spores or other "resting stages" with low metabolic rates. The Arrhenius equation is used to predict the maintenance energy requirement of active microbes as a function of temperature. Decomposition rates, the rates of substrate disappearance, are used to predict the activity level of microbes.

Inactive decomposers are assumed to die at a low constant rate. Active decomposers can be killed by freezing or drying. A fraction of active microbes is assumed to die on the day freezing temperatures are reached. Neither thawing nor prolonged freezing weather increases mortality. Active decomposers die at a constant daily rate as long as the effect of water on the decomposition rate is lower than a preset parameter representing severe moisture stress (Hunt, 1978).

NUTRIENT SUBMODELS

Nitrogen and phosphorus are two of the most important nutrients in the annual grassland. Flows of these nutrients through the system are simulated by modified versions of a nitrogen model developed by Reuss and Innis (1977), and a phosphorus model devised by Cole et al. (1977). Interfacing is described by Cole (1976).

The principal changes from ELM are the separation of producer state variables into legume and nonlegume categories to allow the consideration of symbiotic nitrogen fixation and the generally higher nitrogen concentration of legumes (all producers are aggregated in the ELM nutrient submodels); addition of seed state variable; removal of crowns from the phosphorus submodel of ELM (only annual producers are included in the ELMAGE model); and alteration of parameters used in the ELM nutrient-flow functions.

Phosphorus fertilizer, nitrogen in the form of ammonium or nitrate, or all three may be added to the soil on a specific date through an EVENT routine (Gustafson, 1978). Phosphorus is added to the labile inorganic phosphorus of the top soil layer (described below), and nitrogen (in either or both forms) is apportioned among the top three soil layers in proportion to the biomass of live roots in those layers at the time of fertilization.

Nitrogen submodel

Nitrogen state variables for each of four soil layers are used to represent each of the forms of nitrogen in the soil: legume and nonlegume live-root N, belowground litter (dead roots and decomposers) N, nitrate N, ammonium N, and soil organic N (Fig. 8). The single arrows between these state variables imply the description of four flows, one for each of the soil layers.

The processes of nitrogen movement (i.e., mineralization, immobilization, nitrification, decomposition, root uptake, translocation between roots and shoots, and movement among other producer, consumer, and decomposer compartments) are simulated. The nitrogen content of live-root and live-shoot compartments is altered through the processes of uptake and translocation, respectively. Other movements of nitrogen between the producer, consumer, and decomposer-related compartments are dependent upon the nitrogen concentration of the donor compartment and the flows of biomass, which are determined in the other submodels. For example, when biomass flows from seeds to shoots and roots of producers upon germination, nitrogen flows from the seed N com-

partments to the shoot and root N compartments in amounts equal to the products of the flows of biomass and the nitrogen concentrations of the seeds (the latter are supplied as data inputs for legume and nonlegume producers).

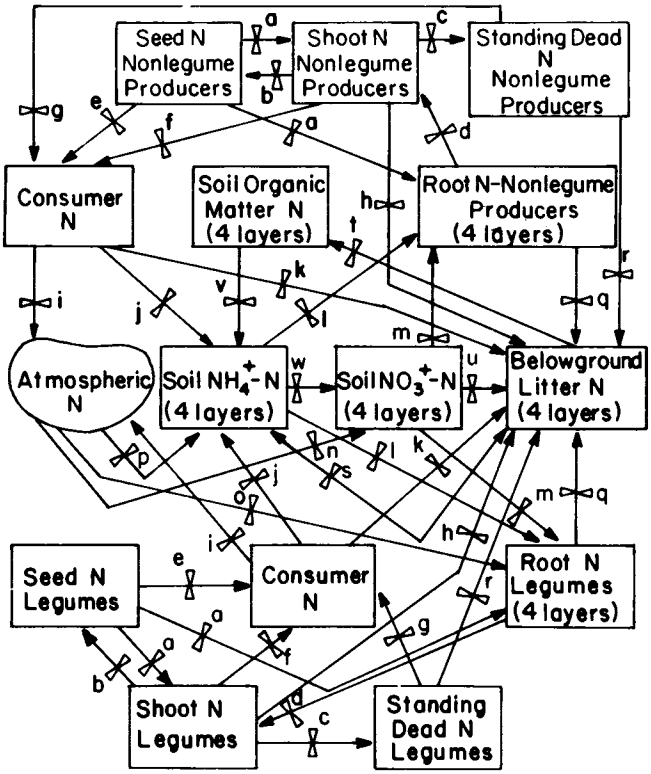

Fig. 8. Flow diagram of nitrogen flows in the nitrogen submodel (modified from Reuss and Innis, 1977).

a. Germination: f (rate of germination, N concentration of seeds).

b. Seed production: f (rate of seed production, N concentration of shoots).

c. Shoot death: f (rate of shoot death, N concentration of shoots).

d. Root-to-shoot translocation: f(N concentration of roots, N concentration of shoots, constant ratio of shoot:root N, phenology).

e. Seed consumption: f (rate of seed consumption, N concentration of seeds).

f. Shoot consumption: f (rate of shoot consumption, N concentration of shoots).

g. Standing-dead plant consumption: f (rate of consumption of standing dead material, N concentration of standing dead plants).

h. Shoot "waste" by consumers: f (rate of shoot-to-litter waste caused by consumption of shoots, N concentration of shoots).

i. Gaseous loss of N by consumers: f (N in consumer waste products, gaseous fraction of consumer waste).

j. Urination N loss by consumers: f(N in consumer waste products, urine fraction in consumer waste).

k. Death and defecation of consumers: f(N in consumer waste products, N in dead consumers, death rate of consumers, fecal fraction of consumer waste).

l. Uptake of NH_4: f (N concentration of soil NH_4, N concentration of roots, effect of soil water, effect of soil temperature, Michaelis-Menten equation constants).

m. Uptake of NO_3: f (N concentration of soil NO_3, N concentration of roots, effect of soil water, effect of soil temperature, Michaelis-Menten equation constants).

n. Atmospheric N to soil NO_3: f(rainfall, NO_3 content of rainfall).

o. Symbiotic N fixation: f (legume root biomass, rate of N fixation by legume roots, photosynthetic activity).

p. Atmospheric N to soil NH_4: f(rainfall, NH_4 content of rainfall, fraction of symbiotically fixed N).

q. Root death: f(rate of root death, N concentration of roots).

r. Fall of standing dead to litter: f(rate of fall of standing dead to litter, N concentration of standing dead).

s. Belowground litter N to NH_4 (mineralization): f(N concentration of belowground litter, decomposition rate, effect of soil water and temperature, and the NH_4-fraction of decomposing material which varies daily as a function of the C/N ratio of the substrate).
NH_4 to belowground litter N (immobilization): f (NH_4 concentration of soil, effect of soil water and temperature, and the immobilization rate which varies as a function of biomass and N concentration of belowground litter).

t. Decomposition: f(N concentration of belowground litter, decomposition rate, soil organic matter N-fraction of decomposing material which varies daily as a function of the C/N ratio of the substrate).

u. Immobilization: f(NO_3 concentration of soil, effect of soil water and temperature, and the immobilization rate which varies as a function of biomass and N concentration of belowground litter).

v. Ammonification: f(soil organic matter N, effect of soil water and temperature, and a rate constant).

w. Nitrification: f(NH_4 concentration of soil, NO_3 concentration of soil, level of microbial activity, and the effect of soil water and temperature).

Some flows of biomass in the other submodels are dependent upon information supplied by the nitrogen submodel. Decomposition rates are a function of both soil and plant nitrogen concentrations. Also, shoot-nitrogen concentrations influence rates of photosynthesis of the producers (as described in the "Producer" section).

Consumer nitrogen flows were included in the submodel solely to provide a mechanism which would not allow nitrogen concentrations of producers to change significantly due to animal consumption of producer biomass. Consumers are assumed to have a constant nitrogen concentration. The excess of nitrogen intake by consumers, beyond that needed to maintain their constant nitrogen concentration, flows from the consumer nitrogen compartment. The flow of excess nitrogen is partitioned in fixed proportion among gas (which flows to the atmospheric sink), feces (which flow to the upper litter compartment), and urine (which flows to the soil ammonium compartment). Upon the death of consumers, nitrogen in dead consumer biomass flows to the upper litter compartment (Reuss and Innis, 1977).

The simulation of symbiotic fixation of nitrogen has been included in the ELMAGE version of the submodel. Up to 10 g $N \cdot m^{-2}$ per year may be added to the soil by clover via this pathway (Milthorpe and Moorby, 1974; Williams et al., 1977). Symbiotic fixation is a function of the biomass of legume roots and an assumed daily rate of symbiotic fixation per g of legume roots. Fixation is only allowed when legumes are photosynthetically active and beyond the seedling stage. Thus, environmental conditions which regulate photosynthesis indirectly influence the rate of symbiotic fixation. Symbiotically

fixed nitrogen is divided between the legume-root nitrogen compartments and the soil ammonium compartments (representing sloughed root material and shed root nodules).

Phosphorus submodel

Phosphorus state variables, one for each of the four soil nutrient layers, represent each of the forms of phosphorus in the soil (Fig. 9). Thus, each of the arrows between these state variables in Fig. 9 represents four flows. Live-root phosphorus is aggregated by depth for legume and nonlegume producers.

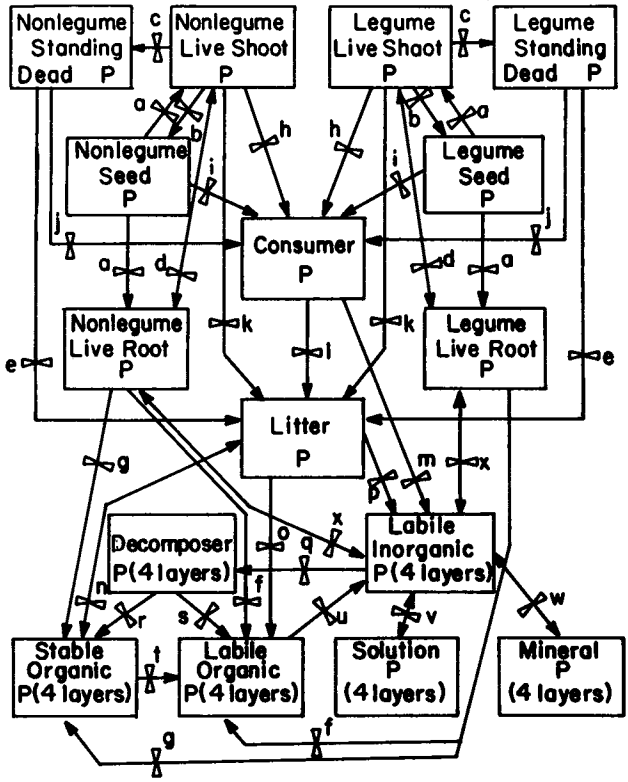

Fig. 9. Flow diagram of phosphorus flows in the phosphorus submodel (modified from Cole, Innis, and Stewart, 1977).

a. Germination: f(rate of germination, P concentration of seeds).

b. Seed production: f(rate of seed production, P concentration of shoots).

c. Shoot death: f(rate of shoot death, P concentration of shoots).

d. Root-to-shoot translocation: f(effect of root P concentration, effect of shoot P concentration, phenology, live shoot biomass, rate constant) (flow may occur in either direction).

e. Fall of standing dead to litter: f(rate of fall of standing dead to litter, P concentration of standing dead).

f. Root death: f(rate of root death, P concentration of roots, assumed labile organic fraction of dead root P).

g. Root death: f(rate of root death, P concentration of roots, assumed stable organic fraction of dead root P.).

h. Shoot consumption: f(rate of shoot consumption, P concentration of shoots).

i. Seed consumption: f(rate of seed consumption, P concentration of seeds).

j. Standing dead plant consumption: f(rate of consumption of standing dead, P concentration of standing dead).

k. Shoot "waste" by consumers: f(rate of shoot-to-litter waste caused by consumption of shoots, P concentration of shoots).

l. Death and defecation of consumers: f(P in consumer waste products, P in dead consumers, death rate of consumers, fecal P fraction of consumer waste).

m. Urination P loss by consumers: f(P in consumer waste products, urine P fraction of consumer waste).

n. Litter addition to stable organic P (physical mixing): f[litter P, temperature (must be > freezing), rate constants].

o. Litter addition to labile organic P (physical mixing): f[litter P, temperature (must be > freezing), rate constants].

p. Litter addition to labile inorganic P (leaching): f[litter P, temperature (must be > freezing), rate constants].

q. Uptake by decomposers: f (solution inorganic P concentration, Michaelis-Menten equation constants, effect of soil temperature, effect of soil water, decomposer biomass, effect of decomposer P concentration).

r. Death of decomposers: f(decomposer P, effect of soil temperature, effect of soil water, rate constant, stable organic P fraction of dead decomposer P).

s. Death of decomposers: f(decomposer P, effect of soil temperature, effect of soil water, rate constant, labile organic P fraction of dead decomposer P).

t. Decomposition: f(stable organic P, effect of soil temperature, effect of soil water, rate constant).

u. Mineralization: f(labile organic P, effect of soil temperature, effect of soil water, rate constant).

v. Solution and adsorption: f(inorganic solution P, labile inorganic P, rate constant for solution to labile inorganic P, rate constant for labile inorganic to solution P).

w. Weathering: f(labile inorganic P, mineral P, rate constants) (this process is not included in present model development and rate constants are set at zero).

x. Uptake by roots: f[solution inorganic P concentration, Michaelis-Menten equation constants, effect of soil temperature, effect of soil water, effect of root N concentration, active live-root biomass, effect of root P concentration, capacity factor (reflecting soil properties affecting P diffusion)].

The objective of this submodel is to represent the processes involved in the movement of phosphorus through the system, including decomposition, mineralization of organic phosphorus, solution and adsorption of phosphorus in the soil, and diffusion processes involved in the supply of phosphorus to plant roots. Most of the flows in this submodel are regulated by rate constants which are based on knowledge of soil characteristics, empirical observations, or assumptions chosen to produce internally consistent flows throughout the system (Cole et al., 1977).

A problem arises in attempting to describe the rapid transformation of some forms of phosphorus given the daily time step of the model. For example, a very rapid equilibrium may exist between phosphorus in solution and labile inorganic phosphorus (Cole and Olsen, 1959*a,b*). The solution pool is replenished from the labile pool many times daily. Daily root uptake from solution under optimal conditions may be 50 times the amount of phosphorus in solution (Cole et al., 1977). The problem is dealt with in the model by allowing uptake by plant roots and decomposers, to come directly from the pool of

labile inorganic phosphorus. Flow rates per unit weight of root or decomposer biomass are a function of solution phosphorus concentration, labile inorganic phosphorus, and effects of soil temperature and water (Cole et al., 1977).

Separate compartments for decomposer phosphorus, and representation of flows into and out of these compartments are included because of evidence that microbes are responsible for a significant proportion of phosporus redistribution through the soil (Hannapel et al., 1964). Large quantities of phosphorus are required by microbes during the decomposition of plant residues. The uptake of phosphorus by decomposers represents the greatest annual movement of phosphorus in this submodel. Rates of flow were derived from various data on the phosphorus concentrations of decomposer species, estimates of microbial populations, and turnover rates (Cole et al., 1977).

As in the nitrogen submodel, movement of phosphorus between producer and consumer-related compartments is a function of phosphorus concentration of the donor compartment and the flows of biomass, which are determined in the other submodels. The principal example of dependence of other submodel functions on the phosphorus submodel is the influence of shoot-phosphorus concentrations on rates of photosynthesis of producers (as described in the "Producer" section).

Consumer phosphorus flows were included solely to provide a mechanism that would not allow phosphorus concentrations of producers to change significantly because of animal consumption of producer biomass, as with nitrogen. Consumers are assumed to have a constant phosphorus concentration. The excess of phosphorus intake by consumers, beyond that needed to maintain their constant phosphorus concentration, flows in fixed proportions as feces (which represent 95 percent of the flows of excess phosphorus and move to the litter compartment) and urine (which flows to the upper compartment of labile inorganic phosphorus). Upon the death of consumers, phosphorus in dead consumer biomass flows to the litter compartment (Cole, 1976).

The nitrogen and phosphorus submodels are an attempt to represent all processes involved in the movement of nitrogen and phosphorus through the annual grassland ecosystem. The processes are complex and many of them are incompletely understood. Simulation of these nutrient cycles should be regarded as a preliminary effort and as a means for evaluating hypotheses regarding nutrient flows in the annual grassland. These submodels are derived from models which were developed for systems of perennial plants—not annuals—in the Great Plains, where climatic conditions and soils differ greatly from those found in California. A number of changes have been made in adapting the submodels for use in this annual grassland. Nevertheless, continued research on nutrient cycling and further effort toward refining model parameters, with particular emphasis on the processes and conditions of the annual grassland, could result in significant improvement of the model. Also, consideration of sulfur flows would greatly enhance the model description of nutrient limitations in the annual grassland ecosystem since sulfur is often deficient there.

MODEL OUTPUT

The usefulness of dynamic simulation models was studied at length by Forrester (1961, 1968). He concluded that a model is sound and defendable if it accomplishes the objectives for which it was developed. The results of simulation runs with various initial conditions are discussed below in relation to how well some of the objectives defined in

the Introduction have been satisfied; principally, how well does the model "...simulate seasonal dynamics of biomass in a representative annual grassland ecosystem?" Data from the San Joaquin Experimental Range for the year beginning on 1 September 1973 have been used to a large extent in developing the model, and are the basis for the simulations and field data comparisons in the following discussion.

Simulated production of the five functional producer groups with the consumers excluded is shown in Fig. 10(a) and in the presence of deer and ground squirrels, but with no livestock in Fig. 10(b). In the latter, initial stocking levels are 10 deer · km^{-2} (25 deer · mi^{-2}) and 7.5 squirrels · ha^{-1}. This is the closest approximation of the ungrazed (by cattle) field situation. Field data for an open upland range site[4] for the three dominant producer groups (early and later grasses and early forbs) at five sampling points during the season are also shown in this figure. As functional groups are aggregates of plant species, confidence intervals for the field data points are not shown, but sampling variability was high. Simulated production of biomass reaches a peak of approximately 3,300 kg · ha^{-1} (Fig. 10b) while the data indicate peak production of 4,600 kg · ha^{-1}. About 70 percent of this difference is due to the difference between simulated and field measured peak production of later grasses, 1,800 kg · ha^{-1} and 2,700 kg · ha^{-1}, respectively. Simulated peak production values for the other two dominant plant categories also are less than those indicated by the field data. However, the dominance of grasses in this year is evident, and the patterns of growth shown by the simulation and the data are quite similar. Field data for summer forbs and legumes are not shown since each produced less than 40 kg · ha^{-1} during the 1973–74 growth year.

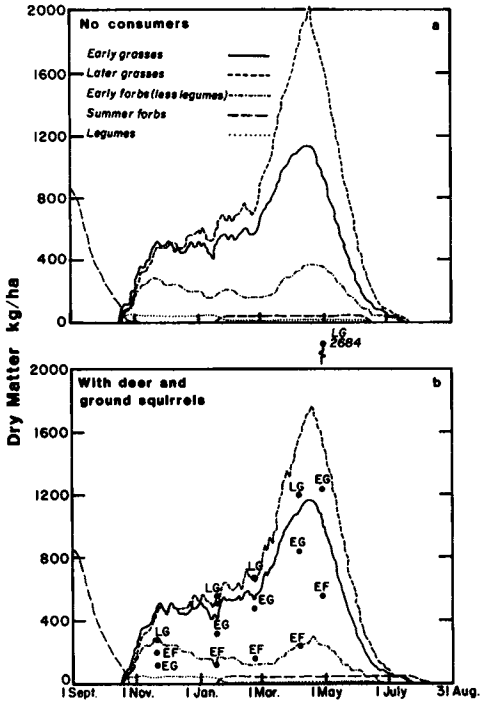

Fig. 10. Simulated live-shoot production of five functional groups of plants with no consumers (a) and with deer and ground squirrels (b). Points indicate field estimates of live-shoot production.

[4] Caldwell, Richard M., John W. Menke, and Donald A. Duncan. Productivity and botanical composition changes in annual grassland as affected by three systems of grazing. Manuscript in preparation.

The date of simulated peak production occurs earlier in each of the three dominant producer groups than indicated by field data for those groups. Also, the pronounced increase in plant growth after the winter cold period occurs earlier in the simulated producers than shown by the field data. This may be partly due to the larger biomass of the simulated producers after the period of germination and establishment. The greater extant leaf area results in plants which are able to gain more immediate advantage from the improvement of environmental conditions after the winter cold period.

The apparent overprediction of production during the germination phase may be due to inaccurate initial conditions or to an inadequate representation of germination and establishment. This period is very important in determining production patterns in annual grasslands. Simulation of germination and seedling mortality may be greatly refined in future modeling efforts as continued research provides more precise information and a better understanding of this critical period.

It should be noted that field data shown in Fig. 10(b) do not represent an absolute standard of yearly production. Production data in a grassland are extremely variable and confidence intervals around such means are large. Given this variability, trends in yearly productivity are as important for comparative purposes as the magnitudes of each of the producers. The model seems to represent trends reasonably in the seasonal dynamics of producer biomass.

Cattle have grazed the San Joaquin Range for many years. Plant production was simulated with cattle grazing at three levels of intensity, approximately one cow per 12, 8, and 6 ha (Fig. 11—a, b, and c, respectively). Deer and ground squirrels, at the numbers specified above, are included in these and all remaining simulations described in this section (i.e., for both grazed and ungrazed conditions). Reproduction of all these consumers, and concomitant increases in grazing intensity, occur during the model year. Fall calving is assumed for the cattle and all calves are born on the same day, 21 October.

Simulated standing crop of the three dominant producer groups at the time of peak standing crop of the plant community are summarized in Table 5 for the ungrazed situation and for three levels of cattle grazing. Standing forage decreased by about 9 percent by cattle grazing at the lowest stocking level. Forage remaining was further decreased by 6–7 percent with each further increase in stocking level.

There were relatively large decreases in peak production with increases in grazing intensity for two of the three dominant producer groups. Later grasses (*Bromus mollis* and miscellaneous grasses) decreased from 1,800 kg · ha $^{-1}$ without grazing to 1,190 kg · ha $^{-1}$ with cattle at stocking level 3. Early forbs (primarily *Erodium* spp.) decreased from 270 kg · ha $^{-1}$ without grazing to 50 kg · ha $^{-1}$ when cattle were stocked at level 3. There was little change in simulated peak production of the early grasses group (*B. diandrus* and *Festuca* spp.) with increases in grazing.

TABLE 5. SIMULATED PEAK STANDING CROP (KG/HA) OF THE THREE DOMINANT PLANT GROUPS WITHOUT GRAZING AND AT DIFFERENT STOCKING LEVELS

	Standing crop production and stocking level*			
Producer group	Ungrazed	(1) 0.083 cow/ha	(2) 0.125 cow/ha	(3) 0.167 cow/ha
		kg/ha		
Early grasses	1,190	1,120	1,230	1,210
Later grasses	1,800	1,510	1,350	1,100
Early forbs (less legumes)	270	210	180	150
Community total	3,320	3,020	2,840	2,640

* Stocking levels: (1) = one cow/30 acres; (2) = one cow/20 acres; (3) = one cow/15 acres.

Grazing had a pronounced effect on production of summer annual forbs. Peak production of this functional group is reached in July, several months later than the rest of the plant community. With no grazing, simulated peak production of summer annuals was less than 50 kg · ha^{-1} (dry weight). When cattle were simulated at grazing level 1, and production of the total plant community was reduced, summer annual forb production increased to about 380 kg · ha^{-1} (Fig. 11). With cattle at stocking levels 2 and 3, summer annual production increased to 790 kg · ha^{-1} and 1,260 kg · ha^{-1}, respectively. With increasing grazing intensity, both production and canopy height of the total plant community decreased. As a result, there was less competition for light, water, and other nutrients during late spring when summer annuals enter a period of greatest potential growth. This producer group is shunned by cattle and is relatively unaffected by increased grazing; thus, these species obtain a relative competitive advantage (Perrier et al. 1982).

Though field data for relative cover are not available, simulated values appear reasonable given the dominance of grasses in 1973–74. At the time of greatest standing crop on ungrazed range, more than 50 percent of simulated plant cover is composed of later grasses, and total grasses comprise more than 85 percent of total cover (Fig. 12, a). The effect of grazing on relative cover is shown in Fig. 12, b; e.g., reduced cover of later grasses reflects the preference of cattle for this group and the dramatic increase in cover of summer annual forbs was due to the enhanced competitive advantage of this group, not preferred by cattle, as discussed above. In this and following comparisons of ungrazed and grazed conditions, grazing was simulated with cattle at stocking level 3.

Root:shoot ratios of approximately 0.5 for annual grasses and as low as 0.23 for winter annual forbs have been reported in the literature (Stern, 1965; Asher and Ozanne, 1966; Gerakis et al., 1975); however, the studies cited involved either plants measured at an early stage of growth, plants grown in the laboratory, or plants in a single-species sward. Estimates of above and belowground components of net production of a mixed annual pasture were made at the San Joaquin Experimental Range in 1974. Root:shoot ratios derived from these estimates, made in two separate studies, were 0.64[5] and 0.72[6]. Simulated root:shoot ratios for the three dominant functional groups of producers (Fig. 13, ungrazed and grazed range) appear reasonable given the ratios cited, which were based on data from similar sites and the same year, 1974. Data on the seasonal dynamics of root:shoot ratios of annual species were not available for comparison with simulated values. Sharp increases in the ratios at the end of the growth season indicate more rapid death of shoots relative to roots as the season ends.

Maximum heights of each of the functional groups of producers under ungrazed and grazed conditions are shown in Figure 14. Relative differences in the effect of grazing on height are due to the degree to which each producer group is preferred by grazing cattle, and are highly correlated with the effect of grazing on plant production. Production of later grasses, for example, was reduced by 34 percent by simulated grazing of cattle at stocking level 3 (Table 5). Maximum height of this group was reduced due to grazing by about the same proportion, from 25 to 16 cm (Fig. 14). Heady (1957) measured average heights of annual grassland species in several ungrazed and grazed sites over several seasons. Maximum heights simulated by the model compare favorably with his data for the same species.

[5] Woodmansee, R. G., D. A. Duncan, D. C. Coleman, and M. K. Campion. Dynamics of roots and soil water in an annual grassland ecosystem. Manuscript in preparation.

[6] Duncan, D. A., and R. G. Woodmansee. Plant biomass, soil water dynamics, and primary production in an annual grassland ecosystem. Manuscript in preparation.

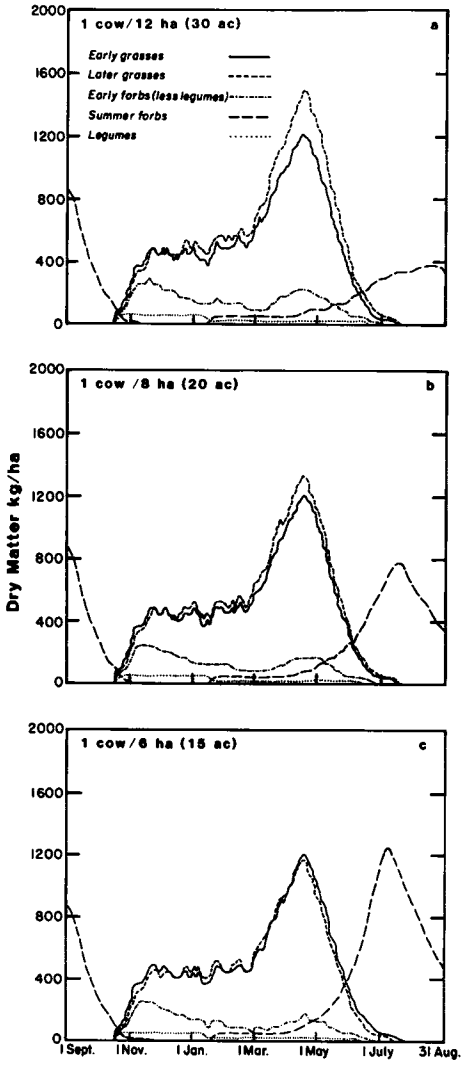

Fig. 11. Simulated live-shoot production of five functional groups of plants with simulated consumption by deer, ground squirrels, and cattle stocked at one cow per 12, 8, and 6 ha (a, b, and c).

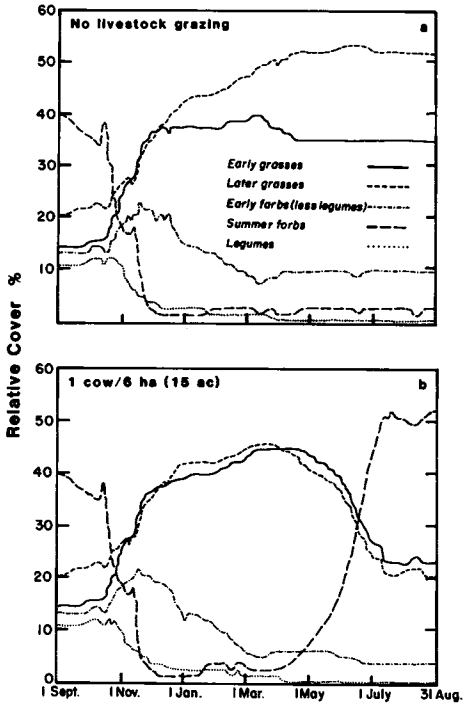

Fig. 12. Simulated relative cover of the standing crop of five functional groups of plants without (a) and with (b) livestock grazing.

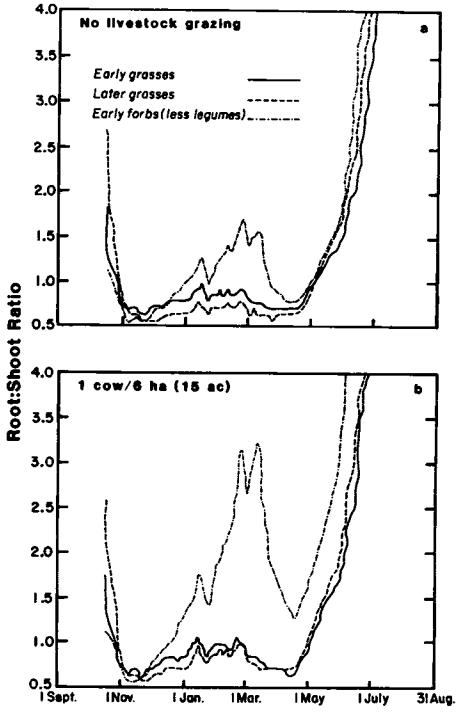

Fig. 13. Simulated root:shoot ratios for three functional groups of plants without (a) and with (b) livestock grazing.

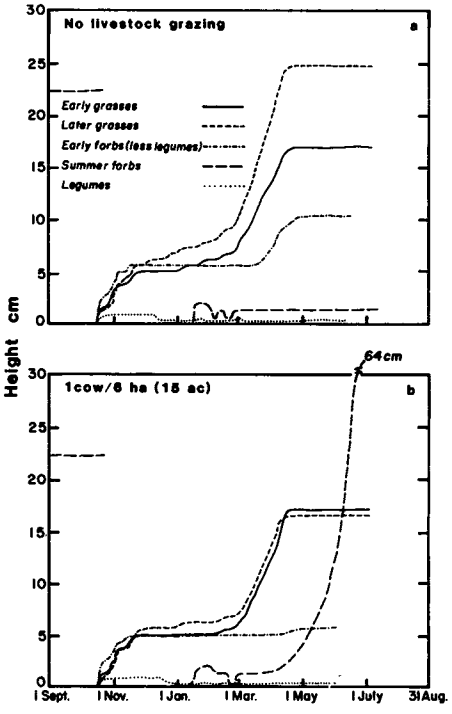

Fig. 14. Simulated maximum height of five functional groups of plants without (a) and with (b) livestock grazing.

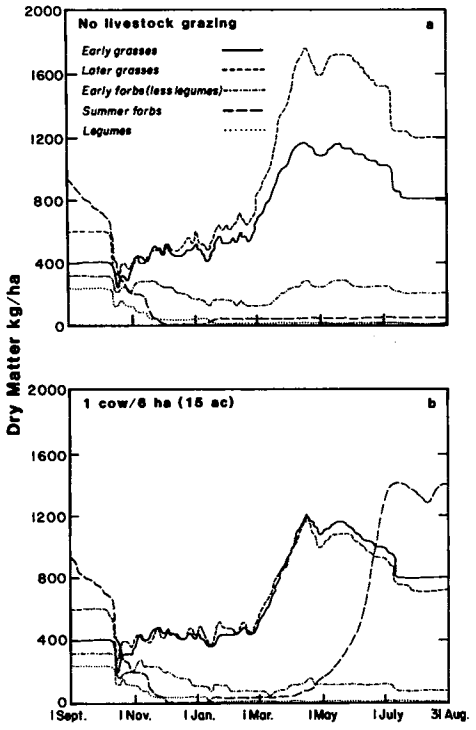

Fig. 15. Simulated standing crop (live shoots and standing dead shoots) of five functional groups of plants without (a) and with (b) livestock grazing.

Range forage available to grazing animals includes erect dead plant material as well as live shoots. Combined live and dead shoot material, the simulated "standing crop," under ungrazed and grazed conditions is shown in Figure 15. During the period of most rapid plant growth, virtually all of the standing crop was composed of live shoots (Figs. 10, 11). Erect dead material at the end of the year decreased from approximately 2,200 kg · ha^{-1} to 1,600 kg · ha^{-1} (excluding summer annual forbs) for ungrazed and grazed range, respectively (Fig. 15). This amount of dead material remaining after simulated grazing (at stocking level 3, one cow · 6 ha^{-1}) suggests that cattle could be stocked more heavily without adverse effects on the plant community. A rule of thumb for the desired amount of residue to be left on annual rangeland following grazing is 750 kg · ha^{-1}.

Total nitrogen accumulated in the shoots of all producers throughout the year, with and without simulated cattle grazing, is shown in Figure 16. The seasonal patterns of total shoot nitrogen were similar in both cases (ungrazed and grazed) and the proportional reduction of peak shoot nitrogen under grazing (about 19 percent) closely corresponded to the proportional reduction of peak shoot biomass under grazing.

Phosphorus and nitrogen concentrations in the shoots and roots of all producers except the legume group are described in Figure 17. Field data for shoot concentrations of phosphorus and nitrogen are included in this value. Average daily shoot phosphorus concentration did not vary greatly over the growth season, and simulated values were in close agreement with field data.

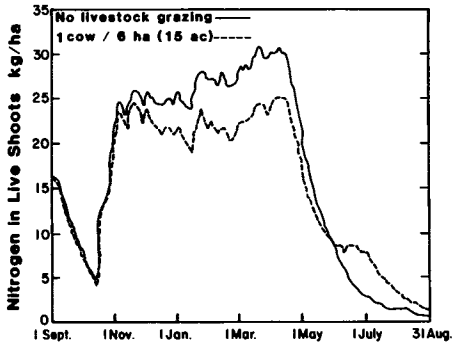

Fig. 16. Simulated nitrogen accumulation in live shoots of all plants with and without livestock grazing.

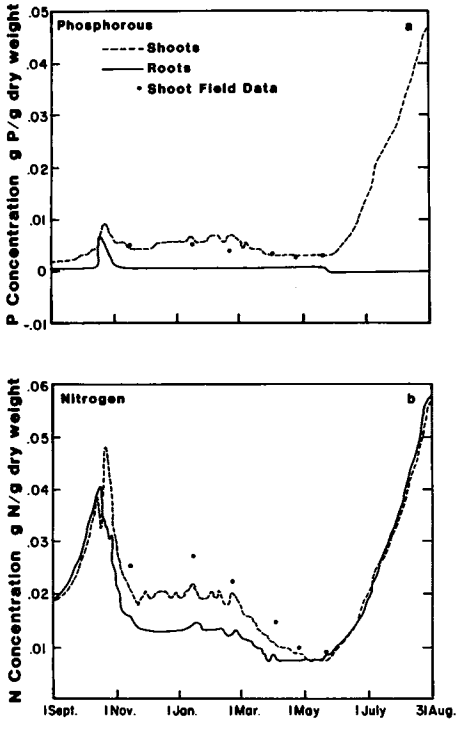

Fig. 17. Simulated phosphorus (a) and nitrogen (b) concentrations in the live shoots and roots of all plants except legumes without livestock grazing. Points indicate field estimates of shoot phosphorus and nitrogen concentrations.

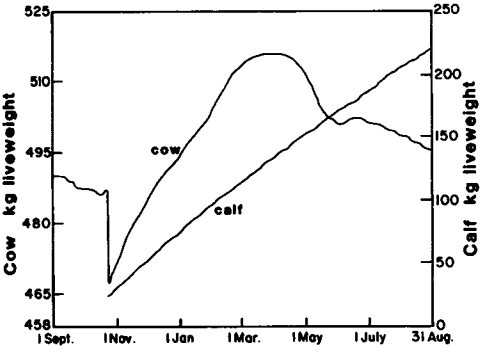

Fig. 18. Simulated average live weights of cows and calves with cattle stocked at one cow per 6 ha.

The seasonal pattern of simulated shoot nitrogen concentration was similar to that measured in the field. Nitrogen concentration was greatest early in the growth season and began to decrease when plants entered a period of most rapid growth with increasing warmth and light in the spring. Simulated nitrogen concentration was less than the field-measured concentration during much of the growth season. This difference, up to 20 percent of the simulated values, cannot be explained. Further work on the nutrient submodels and the interface between these submodels and the producer submodel is needed. In particular, movement of nutrients within the producers and nutrient requirements of the producers during seed synthesis should be studied closely.

Apparent rapid increases in concentrations of shoot phosphorus and shoot and root nitrogen began after plant production had peaked. Producers died relatively rapidly, plant biomass was lost more rapidly than nutrients, and nutrient concentrations appeared to increase greatly. Total plant nutrients during this period actually decreased through the end of the year (Fig. 16).

Primary producers are the principal focus of the ELMAGE model. Consumers have been simulated to study the effects of various intensities of herbivory on primary production. Accurate representation of these effects depends on an adequate model of the changing status of consumers, particularly livestock, throughout the year. The simulated average weight of cows varied between 470 kg following the birth of calves in late October and 520 kg in the spring of the following year (Fig. 18). Cattle gained weight during most of the growth season of plants until a period preceding peak plant production. Following this peak, as the dead plants began to dry and diminish in quality, cattle began to lose weight. Calves gained weight from birth until the end of the year, when their simulated average weight was about 220 kg (Fig. 18).

Only a few of the scores of variables in the model have been included in this brief description of model output. Some aspects of the seasonal dynamics of the annual grassland are represented reasonably by the ELMAGE model while other characteristics of the system are not represented as well. Many functions of the current model may be changed through future efforts to improve the realism of the functions or to allow consideration of specific questions about the system heretofore not considered.

Many hypotheses concerning the structure and function of the annual grassland ecosystem may be formulated with the model through simple changes of input variables, driving variables (weather conditions), or output parameters. A long-term plant production database coupled with the more detailed 3-year IBP data sets (fall 1972—fall 1975) at the San Joaquin Experimental Range will be used in future model development and testing. Though the model was developed and tested with data from this site, simple changes in input data should allow its use for other sites in the California annual grassland. One such application of the model was made at the Sierra Foothill Range Field Station (18 miles ENE of Marysville, California). The model was used to derive coefficients of seasonal forage production for a linear programming model of a cattle operation (Center, 1981). In addition, model functions and output have been used in classes studying the annual grassland ecosystem.

LITERATURE CITED

ALTMAN, P. L., and D. S. DITTMER
1964. Biology data book. Fed. Amer. Soc. Exp. Biol. Washington, D.C.: 633 p.
ANWAY, J. C.
1978. A mammalian consumer model for grasslands, pp. 89–125. *In* G. S. Innis (ed.) Grassland simulation model. New York: Springer-Verlag.
ASHER, C. J., and P. G. OZANNE.
1966. Root growth in seedlings of annual pasture species. Plant and Soil 24: 423–36.
BARTOLOME. J. W.
1976. Germination and establishment of plants in California annual grassland. Ph.D. Dissertation, Univ. Calif., Berkeley. 187 pp.
BENNETT, O. L., and B. D. DOSS.
1960. The effect of soil moisture level on root distribution of cool season forage grasses. Agron. J. 52: 204–07.
BENTLEY, J. R., and M. W. TALBOT.
1951. Efficient use of annual plants on cattle ranges in the California foothills. USDA Circ. No. 870. 52 pp.
BISWELL, H. H., and C. A. GRAHAM.
1956. Plant counts and seed production on California annual-type ranges. J. Range Manage. 9: 116–18.
BLACK, C. A.
1968. Soil-plant relationships. 2nd Ed. New York: Wiley. 792 pp.
BLACK, J.N.
1958. Competition between plants of different initial seed sizes in swards of subterranean clover (*Trifolium subterraneum* L.) with particular reference to leaf area and the light microclimate. Aust. J. Agric. Res. 9: 299–318.
BLACK, T. A., W. R. GARDNER, and G. W. THURTELL.
1969. The prediction of evaporation, drainage and soil water storage for a bare soil. Soil Sci. Soc. Am., Proc. 33: 655–60.
BRENNAN, R. D., C. T. de WIT, W. A. WILLIAMS, and E. V. QUATTRIN.
1970. The utility of a digital simulation language for ecological modeling. Oecologia 4: 113–32.
BRIX, H.
1962. The effect of water stress on the rates of photosynthesis and respiration in tomato plant and loblolly pine seedlings. Physiol. Plant. 15: 10–20.
BRODY, S.
1945. Bioenergetics and growth. New York: Reinhold Publ. Co. New York: 1023 pp.
BROUGHAM, R. W.
1958. Leaf development in swards of white clover (*Trifolium repens* L.). N.Z. J. Agric. Res. 1: 707–18.
BROUWER, R.
1966. Root growth of grasses and cereals, p. 153–66. *In* F. L. Milthorpe and J. D. Ivins (ed.). The growth of cereals and grasses, Proceedings of the 12th Easter School of Agricultural Science, Univ. Nottingham. Butterworths, London.
BROUWER, R., and C. T. de WIT.
1969. A simulation model of plant growth with special attention to root growth and its consequences, p. 224–44. *In* W. J. Whittington (ed.). Root growth, Proceedings of the 15th Easter School of Agricultural Science, Univ. Nottingham. Butterworths, London.
CAMPBELL, C. A., E. A. PAUL, D. A. RENNIE, and K. J. MCCALLUM.
1967. Applicability of the carbon-dating method of analysis to soil humus studies. Soil Sci. 104: 217–24.
CENTER, D. M.
1981. Resource allocation in a Sierra-Nevada foothill beef cow-calf operation through linear programming. Ph.D. Dissertation, Univ. Calif., Davis. 221 pp.
CLARK, F. E., and E. A. PAUL.
1970. The microflora of grasslands. Adv. Agron. 22: 375–435.
COLE, C. V., G. S. INNIS, and J. W. B. STEWART
1977. Simulation of phosphorus cycling in semiarid grasslands. Ecology 58: 1–15.
COLE, C. V., and S. R. OLSEN.
1959*a*. Phosphorus solubility in calcareous soils. I. Dicalcium phosphate activities in equilibrium solutions. Soil Sci. Soc. Am., Proc. 23: 116–18.
1959*b*. Phosphorus solubility in calcareous soils. II. Effects of exchange phosphorus and soil texture on phosphorus solubility. Soil Sci. Soc. Am., Proc. 23: 119–21.
COLE, G. W.
1976. Nutrient submodels, p. 304–97. *In* G. W. Cole (ed.) ELM: version 2.0. Range Sci. Dept. Sci. Ser. No. 20. Colorado State Univ., Fort Collins. 663 p.
CONNOR, D. J., L. F. BROWN, and M. J. TRLICA.
1974. Plant cover, light interception, and photosynthesis of shortgrass prairie—a functional model. Photosynthetica 8: 18–27.

CORBETT, E. S., and R. P. CROUSE
1968. Rainfall interception by annual grass and chaparral. . .losses compared. USDA Forest Serv. Res. Paper PSW-48. 12 pp.
CRAFTS, E. C.
1938. Height-volume distribution in range grasses. J. Forestry 36: 1182–185.
DAVIDSON, R. L.
1969. Effects of soil nutrients and moisture on root/shoot ratios in *Lolium perenne* L. and *Trifolium repens* L. Ann. Bot. 33: 571–72.
de WIT, C. T.
1965. Photosynthesis of leaf canopies. Agric. Res. Rep. No. 663. Centre for Agric. Pub. and Doc. Wageningen, The Netherlands, 57 pp.
DONALD, C. M.
1963. Competition among crop and pasture plants. Adv. Agron. 15: 1–118.
ERICKSON, R. O.
1959. Integration of plant growth processes. Am. Natur. 93:225–35.
FELBECK, G. T., JR.
1971. Chemical and biological characterization of humic matter, p. 36–59. *In* A. D. McLaren and J. Skujins (ed.) Soil biochemistry. Vol. 2. New York: Marcel Dekker, Inc.
FLOATE, M. J. S.
1970. Decomposition of organic materials from hill soils and pastures. II. Comparative studies on the mineralization of carbon, nitrogen and phosphorus from plant materials and sheep faeces. Soil Biol. Biochem. 2: 173–85.
FORRESTER, J. W.
1961. Industrial dynamics. Cambridge, Mass.: The M.I.T. Press. 464 pp.
1968. Principles of systems. Cambridge, Mass.: Wright-Allen Press, 400 pp.
FRIEND, D. J. C.
1965. The effects of light and temperature on the growth of cereals, p. 181–99. *In* J. L. Milthorpe and J. D. Ivins (ed.) The growth of cereals and grasses, Proceedings of the 12th Easter School of Agricultural Science, Univ. Nottingham. Butterworths, London.
FULWOOD, P. G., and D. W. PUCKRIDGE.
1970. Photosynthesis of Wimmera ryegrass (*Lolium rigidum* Gaud.) in the field. Proc. 11th Int. Grassl. Cong. 530–34.
GERAKIS, P. A., F. P. GUERRERO, and W. A. WILLIAMS.
1975. Growth, water relations, and nutrition of three grassland annuals as affected by drought. J. Appl. Ecol. 12: 125–35.
GLADSTONES, J. S., and J. F. LONERAGAN.
1975. Nitrogen in temperate crop and pasture plants. Aust. J. Agric. Res. 26: 103–12.
GORDON, A., and A. W. SAMPSON
1939. Composition of common California foothill plants as a factor in range management. California Agr. Exp. Sta. Bul. 627. 95 pp.
GUSTAFSON, J. D.
1978. SIMCOMP 3.0 (Appendix 1.A.), p. 22–30. *In* G. S. Innis (ed.) Grassland simulation model. New York: Springer-Verlag.
HANNAPEL. R. J., W. H. FULLER, and R. H. FOX.
1964. Phosphorus movement in a calcareous soil: II. Soil microbial activity and organic phosphorus movement. Soil Sci. 97: 421–27.
HARPER, J. L.
1977. Population biology of plants. New York: Academic Press. 892 pp.
HAURWITZ, B.
1941. Dynamic meterology. New York: McGraw-Hill Book Co., Inc. 365 pp.
HEADY, H. F.
1950. Studies on bluebunch wheatgrass in Montana and height-weight relationships of certain range grasses. Ecol. Monogr. 20: 55–81.
1957. The measurement and value of plant height in the study of herbaceous vegetation. Ecology 38: 313–20.
1958. Vegetational changes in the California annual type. Ecology 39: 402–16.
HESS, S. L.
1959. Introduction to theoretical meterology. New York: Holt. 362 pp.
HUNT, H. W.
1976. Overview of ELM, pp. 5–11. *In* G. W. Cole (ed.) ELM: version 2.0. Range Sci. Dept. Sci. Ser. No. 20. Colorato State Univ., Fort Collins. 663 pp.
1978. A simulation model for decomposition in grasslands. p. 155–84. *In* G. S. Innis (ed.) Grassland simulation model. New York: Springer-Verlag.
HUNT, W. F.
1971. Leaf death and decomposition during pasture regrowth. N.Z. J. Agric. Res. 14: 208–18.

INNIS, G. S. (ed.)
1978. Grassland simulation model. New York: Springer-Verlag. 298 pp.
JONES, M. B.
1963. Yield, percent nitrogen, and total nitrogen uptake of various California annual grassland species fertilized with increasing rates of nitrogen. Agron. J. 55: 254–57.
JONES, M. B., J. E. RUCKMAN, and P. W. LAWLER
1972. Critical levels of P in subclover (*Trifolium subterraneum* L.). Agron. J. 64: 695–98.
KRAMER, P. J.
1969. Plant and soil water relationships: a modern synthesis. New York: McGraw-Hill Inc. 482 pp.
LAUDE, H. M.
1956. Germination of freshly harvested seed of some western range species. J. Range Manage. 9: 126–29.
LEMON, E. R.
1956. The potentialities for decreasing soil moisture evaporative loss. Soil Sci. Soc. Am., Proc. 20: 120–25.
LOOMIS, R. S., and W. A. WILLIAMS
1963. Maximum crop productivity: an estimate. Crop Sci. 3: 67–72.
LUDLOW, M., and G. WILSON
1971. Photosynthesis of tropical pasture plants. I. Illuminance, carbon dioxide concentration, leaf temperature, and leaf-air vapour pressure difference. Aust. J. Biol. Sci. 24: 449–70.
MARTIN, W. E.
1958. Sulfur deficiency widespread. Calif. Agric. 12: 10–12.
MCCOWN, R. L., and W. A. WILLIAMS
1968. Competition for nutrients and light between the annual grassland species *Bromus mollis* and *Erodium botrys*. Ecology 49: 981–90.
MCCREE, K. J.
1970. An equation for the rate of respiration of white clover plants grown under controlled conditions, p. 221–29. *In* I. Setlik (ed.) Prediction and measurement of photosynthetic productivity. Proc. IBP/PP Tech. meeting, Trebon. Centre for Agric. Publ. and Doc., Wageningen.
MCGOWAN, A. A., and W. A. WILLIAMS
1971. Growth of subterranean clover established with a cereal companion crop. Agron. J. 63: 643–46.
MCKELL, C. M., M. B. JONES, and E. R. PERRIER
1962. Root production and accumulation of root material on fertilized annual range. Agron. J. 54: 459–62.
MILTHORPE, F. L., and J. MOORBY
1974. An introduction to crop physiology. London: Cambridge Univ. Press. 202 pp.
MOEN, A. N.
1973. Wildlife ecology. San Francisco: W. H. Freeman & Company. 458 pp.
MOONEY, H. A., R. D. WRIGHT, and B. P. STRAIN
1964. The gas exchange capacity of plants in relation to vegetation zonation in the white mountains of California. Am. Midl. Nat. 72: 281–97.
MUNN, R. E.
1966. Descriptive micrometeorology. New York: Academic Press, Inc. 245 pp.
OZANNE, P. G., J. KEAY, and E. F. BIDDISCOMBE
1969. The comparative applied phosphate requirements of eight annual pasture species. Aust. J. Agric. Res. 20: 809–18.
PARTON, W. J.
1978. Abiotic section of ELM, p. 31–54. *In* G. S. Innis (ed.) Grassland simulation model. New York: Springer-Verlag.
PENMAN, H. L.
1948. Natural evaporation from open water, bare soil and grass. Royal Soc. (London), Proc. A. 193: 120–45.
PERRIER, G. K., W. A. WILLIAMS, and J. W. MENKE
1982. Tarweed, an unloved annual-type range plant. Rangelands 4: 149–50.
PETERS, D. B., and J. R. RUNKLES
1967. Shoot and root growth as affected by water availability, p. 373–89. *In* R. M. Hagan, H. R. Haise and T. W. Edminister (ed.) Irrigation of agricultural lands. American Society of Agronomy Monogr. No. 11, Madison, WI.
REUSS, J. O., and G. S. INNIS
1977. A grassland nitrogen flow simulation model. Ecology 58: 379–88.
ROBSON, M. J.
1973. The growth and development of simulated swards of perennial ryegrass. I. Leaf growth and dry weight change as related to the ceiling yield of a seedling sward. Ann. Bot. 37: 387–500.
ROSS, M. A., and J. L. HARPER
1972. Occupation of biological space during seedling establishment. J. Ecol. 60: 77–88.
ROSSITER, R. C.
1966. Ecology of the Mediterranean annual-type pasture. Adv. Agron. 18: 1–56.

RYLE, G. J. A.
1965. Physiological aspects of seed yield in grasses, p. 106–18. *In* F. L. Milthorpe and J. D. Ivins (ed.). The growth of cereals and grasses. Proceedings of the 12th Easter School of Agricultural Science, Univ. Nottingham. Butterworths, London.
SAUER, R. H.
1978. A simulation model for grassland primary producer phenology and biomass dynamics p. 55–88. *In* G. S. Innis (ed.) Grassland simulation model. New York: Springer-Verlag.
SELIGMAN, N. G., H. VAN KEULEN, and J. GOUDRIAAN
1975. An elementary model of nitrogen uptake and redistribution by annual plant species. Oecologia 21: 243–61.
SELLERS, W. D.
1965. Physical climatology. Chicago: Univ. Chicago Press. 272 pp.
SINGH, B. N., and K. N. LAL
1935. Investigations of the effect of age on assimilation of leaves. Ann. Bot. 49: 291–307.
SMITH, C. G., and W. A. WILLIAMS
1973. Model development for a deferred-grazing system. J. Range Manage. 26: 454–60.
STERN, W. R.
1965. The effect of density on the performance of individual plants in subterranean clover swards. Aust. J. Agric. Res. 16: 541–55.
STERN, W. R. and C. M. DONALD.
1962. Light relationships in grass-clover swards. Aust. J. Agric. Res. 13: 599–614.
THORNE, G. N.
1966. Physiological aspects of grain yield in cereals, p. 88–105. *In* F. L. Milthorpe and J. D. Ivins (ed.) The growth of cereals and grasses. Proceedings of the 12th Easter School of Agricultural Science, Univ. Nottingham. Butterworths, London.
WILLIAMS, W. A.
1963. Competition for light between annual species of *Trifolium* during the vegetative phase. Ecology 44: 475–85.
WILLIAMS, W. A., J. N. BLACK, and C. M. DONALD.
1968. Effect of seed weight on the vegetative growth of competing annual *Trifolium*. Crop Sci. 8: 660–63.
WILLIAMS, W. A., M. B. JONES, and C. C. DELWICHE
1977. Clover N-fixation measurement by total-N difference and ^{15}N A-values in lysimeters. Agron. J. 69: 1023–24.
YOUNG, J. A., R. A. EVANS, and B. L. KAY
1970. Germination characteristics of range legumes. J. Range Manage. 23: 98–103.
1973. Temperature requirements for seed germination in an annual-type rangeland community. Agron. J. 65: 656–59.